IN SEARCH OF LOCAL SINGULARITIES IN IDEAL POTENTIAL FLOWS WITH FREE SURFACE

JIAN-GUO LIU

Department of Physics and Department of Mathematics
Duke University, Durham, NC 27708, USA

ROBERT L. PEGO

Department of Mathematical Sciences and Center for Nonlinear Analysis
Carnegie Mellon University, Pittsburgh, Pennsylvania, PA 12513, USA

Abstract. For ideal fluid flow with zero surface tension and gravity, it remains unknown whether local singularities on the free surface can develop in well-posed initial value problems with smooth initial data. This is so despite great advances over the last 25 years in the mathematical analysis of the Euler equations for water waves. Here we expand our earlier work (*Chin. Ann. Math. Ser. B* 40 (2019) 925) and review the mathematical literature and some of the history concerning Dirichlet's ellipsoids and related hyperboloids associated with jet formation and "flip-through," "splash singularities," and recent constructions of singular free surfaces that however violate the Taylor sign condition for linear well-posedness. We illustrate some of these phenomena with numerical computations of 2D flow based upon a conformal mapping formulation (whose derivation is detailed and discussed in an appendix). Additional numerical evidence strongly suggests that corner singularities may form in an unstable self-similar way from specially prepared initial data.

Contents

E-mail addresses: jliu@phy.duke.edu, rpego@cmu.edu.

Date: July 31, 2021.

2010 *Mathematics Subject Classification.* 76B07,76B10,35L67,30C30.

Key words and phrases. incompressible flow, water wave equations, splash singularity, flip-through, Dirichlet hyperbolas, conformal mapping.

1. Introduction

The highly nonlinear behavior of fluids is an endless source of fascination and challenges to our understanding. Much mathematical analysis can only deal with models of smooth, rather quiescent flows. Yet some of the most powerful and dramatic fluid phenomena are associated with singular flows. What happens when waves crash against a seawall? How do whitecaps form on windblown waves? How do droplets shatter and become spray?

Our understanding of such phenomena is very primitive. We consider here the question of singularity formation for one of the simplest fluid models, Euler's equations for potential flow of an ideal fluid. With velocity field $v = \nabla\phi$, pressure p, and constant density $\rho = 1$, occupying a region $\Omega_t \subset \mathbb{R}^d$ with smooth boundary at time t, these equations take the following form: For each time t,

$$\Delta\phi = 0 \quad \text{in } \Omega_t, \tag{1}$$

$$\phi_t + \frac{1}{2}|\nabla\phi|^2 + p = 0 \quad \text{in } \Omega_t, \tag{2}$$

$$p = 0 \quad \text{on } \partial\Omega_t. \tag{3}$$

The *kinematic condition*, stating that the fluid domain Ω_t is transported by the velocity, supplements these equations. The effects of gravity and surface tension are neglected. At the small scales involved in singularity formation, it is generally appreciated that the effect of gravity ought to be negligible. It is true that surface tension is physically important on small scales, but we focus this study on the mathematical issues that arise when it is neglected.

It is our purpose here to extend our previous work [40] reviewing research relevant to the issue of whether and how local singularities can form in solutions of this system, and offer additional numerical evidence that suggests a new scenario for formation of a local singularity. In the sequel, particularly when considering bounded domains Ω_t we refer to (1)–(3) simply as the *ideal droplet equations*.

2. Background—scenarios for singularities

Mathematical analysis of the initial-value problem for the governing equations (1)–(3) with free boundary is subtle and difficult. The problem can be treated, however, by the methods that S. Wu developed in the 1990s for water waves with gravity. For smooth enough initial data in smooth bounded domains, the works [38, 15, 16] establish short-time existence for

smooth solutions of the incompressible Euler equations with pressureless free boundary in zero gravity, including the case of nonzero vorticity.

In this section we briefly review work related to a number of scenarios for the possible breakdown of smooth solutions and development of singularities in solutions. Bounds that constrain local singularity formation have been provided in recent work of Kinsey and Wu [34] and Wu [61]. In the latter work it is also shown that certain kinds of corners in the free surface can persist for short time if they are present in the initial data.

Splash singularities. A simple way that fluids can develop a singularity is by collision of distinct droplets. A related but more complicated scenario is that different parts of the surface of a connected fluid domain may collide, while the interface remains smooth up to the time of collision. The existence of such *splash singularities* was proved by Castro et al. [8, 7].

Droplet splitting. One can imagine that a single dumbbell-shaped droplet provided with a strongly bipolar initial velocity should break in pieces. There are many physical studies of this behavior that take into account surface tension and/or viscosity. We are not aware of any study of the problem in the absence of these effects, however, and it may be that surface tension is necessary after all for pinch-off to occur. One idea for approaching the splitting problem could involve finding a *least-action* path of fluid configurations that deform one droplet into two. Smooth incompressible potential flows in a fixed domain were shown by Brenier [5, Theorem 2.4] to truly minimize action for sufficiently short time. These flows correspond to volume-preserving paths of diffeomorphisms that minimize distance according to a relaxed version of Arnold's variational characterization of geodesic paths in the diffeomorphism group [1]. It was recently proved, however, that free-boundary flows with zero gravity and surface tension are critical paths for action, but *never minimize it* except for piecewise-rigid motions [41, Corollary 5.6].

Flip-through and jet formation. The breaking of gravity waves against a vertical wall can be thought of as a kind of splash singularity, by reflecting the fluid motion through the plane of the wall. In work of Cooker and Peregrine [13, 14] 2D numerical computations show that wave impacts that trap a bubble of 'air' are less violent than waves that only get *close* to breaking at the wall. Strong forces and very large accelerations can be produced as a sheet of water "flips through" the trough and generates a powerful upward jet of fluid. For discussion of the flip-through phenomenon and related experiments see [53, 4, 58].

In a series of papers including [42, 43, 44, 45], Longuet-Higgins described a jet-formation phenomenon that appears to be associated with flip-through and some other situations where the naïve expectation is that local singularities might form. In particular, Longuet-Higgins described "Dirichlet hyperboloid" exact solutions, extending a family of time-dependent ellipsoidal solutions found by Dirichlet [18] in relation to a long line of investigations on ellipsoidal self-gravitating fluid bodies. As Longuet-Higgins mentioned, Fritz-John [30] had found related flows with parabolic free boundary.

Longuet-Higgins compared Dirichlet hyperboloid solutions with experiments on breaking waves and bubbles in [45]. All the flows he observed remain smooth. There are Dirichlet hyperboloid solutions that become singular in finite time, but what happens is that the pressure and velocity blow up everywhere while the fluid interface remains smooth. By taking a large-scale limit, in [44] Longuet-Higgens described time-dependent solutions that have corners for all times.

Self-similar approach to cones or corners. The tendency to form jets with smooth tips may make it unlikely that smooth free boundaries develop local singularities in many typical flows. We might expect that a local singularity may appear in a borderline situation, e.g.,

between strong flip-through and bubble-trapping splash singularity. Experimental and numerical evidence of such a singularity, for 3D incompressible flows with viscosity and surface tension, was provided by D. Lathrop's group in the 1990s [26, 64]. These authors demonstrated a self-similar collapse of the fluid interface to one with a conical singularity, followed by the dramatic emergence of a very high and thin self-similar jet. No rigorous mathematical analysis of this problem has yet appeared, as far as we are aware.

Ballistic interfaces. In the papers [32, 33], Karabut and Zhuravleva described several analytical solutions of the free-boundary problem (1)–(3) for which fluid particles on the free surface move with *zero acceleration*, i.e., they move ballistically. Very recently, Zubarev and Karabut [66] and Zhuravleva et al. [65] have described examples of this type of flow capable of developing local singularities from a smooth interface. These solutions are derived using the complex Hopf equation by imposing a particular relation between pressure and velocity at the free boundary. Zakharov [63] has provided an interesting independent perspective on solutions of this type.

At present it seems doubtful that the singularities of the kind found in these works can emerge in smooth flows in bounded domains. For acceleration-free interfaces, both the pressure and its gradient vanish at the free boundary. In addition, the pressure-velocity relations imposed in [66, 65] imply that the pressure $p < 0$ inside the fluid domain.

However, it is necessary that $p > 0$ inside the fluid for any nontrivial smooth solution of (1)–(3) in a bounded domain. This follows from the fact that $-\Delta p = \Delta|\nabla\phi|^2 \geq 0$. Then Hopf's lemma implies that

$$\frac{\partial p}{\partial n} < 0 \quad \text{on } \partial\Omega_t. \tag{4}$$

In the present context this says that the *Taylor sign condition* for linear well-posedness holds. More generally this condition requires the outward normal acceleration of the interface to exceed the acceleration due to gravity, see [57, 2]. It was recognized to be key to nonlinear well-posedness theory by Wu [59, 60].

Plan of the paper. In sections 3–5 below, we aim to describe the explicit Dirichlet ellipsoid and hyperboloid solutions of the ideal droplet equations (1)–(3), with a view to focus on their significance for the droplet splitting and jet formation scenarios mentioned above. These solutions exist in an historical context that is interesting to review, involving Hamilton's least action principle, kinematically constrained geodesic flow, and a nontrivial symmetry exhibited by self-gravitating bodies that was made explicit by Dekekind when preparing Dirichlet's work for posthumous publication.

In section 6, we summarize how local singularities on ballistic interfaces were derived in [66] for purely horizontal surface motions and in [65] for cavity collapse scenarios.

Then in the last section below, we extend our computations from [40] to provide additional evidence for a scenario involving unstable corner formation. We make use of a conformal mapping formulation of the governing equations closely related to one described by A. I. Dyachenko in [20] and used by S. A. Dyachenko in [23] to compute bounded ideal droplet solutions with and without surface tension. We find evidence for the existence of a two-parameter of self-similar smooth flows that may emerge from an infinite perfect wedge-shaped domain with power-law initial velocity, by computing a time-reversed flow that develops from a smooth bounded approximation to the wedge, together with a scaling argument. The problem of rigorously demonstrating the existence of such solutions (or showing that some other instabilities must occur on scales invisible to our numerics) appears to pose a difficult challenge for mathematical analysis.

3. Least action principle with free boundary and self-interaction energy

We begin our study by using Hamilton's least action principle, and a variant of the standard Helmholtz decomposition of vector fields, to provide a simple derivation of the governing equations for smooth ideal fluid flows with pressureless free boundary and self-interaction energy. We recall V. I. Arnold's classic use of least action to formally characterizes solutions of the Euler equations for incompressible flows in a fixed domain in terms of geodesic paths of diffeomorphisms.

Let $\Omega_t \subset \mathbb{R}^d$ denote the domain occupied by the fluid at time t, and let X denote the Lagrangian flow map, defined on the space-time domain $Q = \cup_t \Omega_t \times \{t\}$ so that

$$\dot{X}(z,t) = v(X(z,t),t), \qquad X(z,0) = z \in \Omega_0 \tag{5}$$

for all t in some interval $[0,\bar{t}]$. Here the velocity field v is presumed to be sufficiently smooth up to the boundary. The associated density field ρ with given constant initial density ρ_0 is given by

$$\rho(x,t) = \rho_0 \det\left(\frac{\partial X}{\partial z}(z,t)\right)^{-1}, \qquad x = X(z,t) \in \Omega_t. \tag{6}$$

We let $\mathcal{A} = \mathcal{K} - \mathcal{V}$ denote the Lagrangian action associated with the flow, where

$$\mathcal{K} = \frac{1}{2}\int_0^{\bar{t}} \int_{\Omega_t} \rho(x,t)|v(x,t)|^2\,dx\,dt = \frac{1}{2}\int_0^{\bar{t}} \int_{\Omega_0} \rho_0 |\dot{X}(z,t)|^2\,dz\,dt, \tag{7}$$

$$\mathcal{V} = \frac{1}{2}\int_0^{\bar{t}} \int_{\Omega_t^2} \Phi(x,x')\rho(x,t)\rho(x',t)\,dx\,dx'\,dt \tag{8}$$

respectively denote kinetic energy and self-interaction energy with symmetric kernel $\Phi(x,x')$, given for the Newtonian gravitational potential in particular by

$$\Phi(x,x') = -\frac{G}{|x-x'|}.$$

For any family $\varepsilon \to X_\varepsilon$ of flow maps depending smoothly on a variational parameter ε, one finds that the variation $\delta X = (\partial X/\partial\varepsilon)|_{\varepsilon=0}$ induces a density variation $\delta\rho$ satisfying

$$-\frac{\delta\rho}{\rho} = \nabla\cdot\tilde{v}, \qquad \tilde{v}(x,t) = \delta X(z,t),$$

so naturally $\nabla\cdot\tilde{v} = 0$ for variations that leave the density invariant.

We proceed to compute the variation of the action at a density-preserving flow for density-preserving variations. Firstly, requiring that the variation δX *vanishes at the endpoints* $t = 0$ *and* $\bar{t}$, we find

$$\begin{aligned}
\delta\mathcal{K} &= \int_0^{\bar{t}} \int_{\Omega_0} \rho_0 \dot{X}(z,t)\cdot\delta\dot{X}(z,t)\,dz\,dt = -\int_0^{\bar{t}} \int_{\Omega_0} \rho_0 \ddot{X}(z,t)\cdot\delta X(z,t)\,dz\,dt \\
&= -\int_0^{\bar{t}} \int_{\Omega_t} \rho_0(\partial_t v + v\cdot\nabla v)\cdot\tilde{v}\,dx\,dt, \\
\delta\mathcal{V} &= -\int_0^{\bar{t}} \int_{\Omega_t} \rho_0 f(x,t)\cdot\tilde{v}(x,t)\,dx\,dt,
\end{aligned}$$

where $f(x,t)$ is the (specific) self-interaction force field, given by

$$f = -\nabla\varphi, \qquad \varphi(x,t) = \int_{\Omega_t} \rho_0\Phi(x,x')\,dx'.$$

Now a flow X is critical for the action $\mathcal{A}$ if the variation

$$\delta A = \delta K - \delta V = -\int_0^{\bar{t}} \int_{\Omega_t} \rho_0(\partial_t v + v \cdot \nabla v - f) \cdot \tilde{v}\, dx\, dt = 0,$$

for all virtual displacements $\tilde{v}$ for which $\nabla \cdot \tilde{v} = 0$ in Ω_t and which vanish at $t = 0$ and $\bar{t}$. At this point we note that any L^2 vector field u on Ω_t has a unique L^2-orthogonal decomposition

$$u = w + \nabla p, \qquad \text{with} \quad \nabla \cdot w = 0 \ \text{ in } \Omega_t, \quad p = 0 \ \text{ on } \partial\Omega_t, \tag{9}$$

obtained by solving $\Delta p = \nabla \cdot u$ for p in the Sobolev space $H_0^1(\Omega_t)$. (This is a variant of the standard Helmholtz decomposition, see [17, p. 215].) By choosing $u = f - (D_t v + v \cdot \nabla v)$, we infer that for a density-preserving critical path, the velocity field should satisfy the Euler equations

$$\partial_t v + v \cdot \nabla v + \nabla p = f, \quad \nabla \cdot v = 0 \ \text{ in } \Omega_t, \tag{10}$$

with the condition

$$p = 0 \ \text{ on } \partial\Omega_t \tag{11}$$

on the free boundary, along with the *kinematic* condition that $\Omega_t = X(\Omega_0, t)$.

It will be useful below to note that in terms of the deformation gradient $F = \partial X/\partial z$, Euler's equations (10) in Lagrangian coordinates take the form

$$F^T \ddot{X} + \nabla \tilde{p} + \nabla \tilde{\varphi} = 0, \qquad \det F = 1, \tag{12}$$

where $\tilde{p}(z,t) = p(X(z,t),t)$ and $\tilde{\varphi}(z,t) = \varphi(X(z,t),t)$ respectively represent the pressure and force potential in Lagrangian coordinates, since by the chain rule, e.g.,

$$\frac{\partial \tilde{p}}{\partial z} = \frac{\partial p}{\partial x}\frac{\partial X}{\partial z} \qquad \text{so} \quad \nabla \tilde{p} = F^T \nabla p.$$

4. Self-gravitation and Dirichlet's symmetry

In an effort to understand the shape of the earth and other celestial bodies, many prominent investigators, starting with Isaac Newton, have studied the shape of a rotating body of fluid with self-gravitation. Much historical information on this topic can be found in the book of Chandrasekhar [11].

In particular, Dirichlet, in a posthumously published paper edited by Dedekind, was the first to develop equations for *time-dependent* motions that preserve ellipsoidal shape [18]. Of the numerous interesting developments following Dirichlet's work, we mention only a few. From Dirichlet's equations, Dedekind explictly deduced a surprising symmetry, and used it to find ellipsoids with nontrival internal flows, conjugate to the rigidly rotating fluid ellipsoids discovered earlier by Jacobi. In a remarkable paper, Riemann subsequently showed that all rotating, shape-preserving ellipsoids fall into three simple classes, and initiated a study of their stability by energy critera [55].

The reason we bring up this subject is to describe how Dirichlet's ellipsoidal motions can be characterized by through a finite-dimensional least-action principle, and to thereby provide a simple derivation of Dedekind's symmetry. The first descriptions of a reduced least-action principle for Dirichlet ellipsoids appeared only a few years after Riemann's work, in papers by Padova [51] and Lipschitz [39]; see the excellent review by Borisov et al. [3]. In the absence of gravitation, critical paths of action correspond to constant-speed geodesic motion on a determinant-constrained surface in the space of matrices describing the deformation, as noted by O. M. Lavrenteva [36].

We proceed to details. Following Dirichlet, we seek motions for which the domain $\Omega_t \subset \mathbb{R}^3$ is ellipsoidal, with time-dependent semi-axes $a_j(t)$, $j = 1, 2, 3$, having a constant product $a_1 a_2 a_3$. We require the Lagrangian map $z \mapsto X(z,t)$ to be linear, taking the convenient form

$$X_i(z,t) = \sum_{j=1}^{3} P_{ij}(t) \frac{z_j}{a_j(0)}, \qquad z \in \Omega_0, \tag{13}$$

or in more succinct matrix-vector form,

$$X(z,t) = P(t)\Lambda_0^{-1} z, \quad \Lambda_t = \operatorname{diag}\{a_j(t) : j = 1, 2, 3\}. \tag{14}$$

We presume the initial ellipsoid is $\Omega_0 = \Lambda_0 B_1$, where B_1 is the unit ball. That is, $z \in \Omega_0$ if and only if $z = \Lambda_0 y$ with $y \in B_1$. After a rotation of coordinates, $X(z,t)$ should lie in $\Lambda_t B_1$. Thus there should exist orthogonal matrices $R(t)$ and $S(t)$ such that

$$X(z,t) = R(t)\Lambda_t S(t)^T y, \quad \text{with } y = \Lambda_0^{-1} z. \tag{15}$$

The modern eye will recognize that this provides the *singular value decomposition*

$$P = R\Lambda S^T, \quad RR^T = I = SS^T,$$

with the semi-axes a_j being the singular values of P. The matrix $P(t)$ should satisfy

$$P(0) = \Lambda_0 \quad \text{and} \quad \det P(t) = a_1 a_2 a_3 = \text{ constant}. \tag{16}$$

The deformation gradient will be a function of time alone, taking the form

$$F(t) = \frac{\partial X}{\partial z}(z,t) = P(t)\Lambda_0^{-1}. \tag{17}$$

Substituting into Euler's equations written in Lagrangian coordinates, we require

$$F^T \ddot{F} z + \nabla \tilde{p} + \nabla \tilde{\varphi} = 0, \tag{18}$$

where $\tilde{p}$ here is pressure divided by mass density.

It is a remarkable fact, due to Gauss and Rodrigues (see [11, 25]) that the self-gravitation potential is quadratic in the spatial variables, taking the following form. With respect to the coordinates $\hat{x} = R^T x$ taken along the principal axes of the ellipsoid,

$$\varphi(x,t) = -G\rho_0 \pi \, a_1 a_2 a_3 \left(\alpha_0 - \sum_{i=1}^{3} \alpha_i \hat{x}_i^2 \right), \tag{19}$$

$$\alpha_0 = \int_0^\infty \frac{du}{\Delta}, \qquad \alpha_i = -\frac{1}{a_i}\frac{\partial \alpha_0}{\partial \alpha_i} = \int_0^\infty \frac{du}{\Delta(a_i^2 + u)}, \qquad \Delta^2 = \prod_{i=1}^{3} (a_i^2 + u). \tag{20}$$

In Lagrangian variables, using (15) and noting $R^T X = \Lambda S^T \Lambda_0^{-1} z$ we may then write

$$\tilde{\varphi}(z,t) = -G\rho_0 \pi (\alpha_0 + z^T Q z) \det \Lambda \tag{21}$$

where

$$Q = \Lambda_0^{-1} S \Lambda \frac{\partial \alpha_0}{\partial \Lambda} S^T \Lambda_0^{-1}, \quad \frac{\partial \alpha_0}{\partial \Lambda} = \operatorname{diag}\left\{ \frac{\partial \alpha_0}{\partial \alpha_i} \right\}. \tag{22}$$

Then the Lagrangian potential gradient is linear in z, with

$$\nabla \tilde{\varphi}(z,t) = -2G\rho_0 \pi (\det \Lambda)\, Q z \tag{23}$$

In light of (18), the pressure must be quadratic in the spatial variables. In order to vanish on the ellipsoid boundary, it must therefore be that for some scalar function $\beta(t)$,

$$\tilde{p}(z,t) = \frac{1}{2}\beta(t)(1 - |\Lambda_0^{-1} z|^2) \quad \text{and} \quad \nabla \tilde{p}(z,t) = -\beta(t)\Lambda_0^{-2} z. \tag{24}$$

Substituting the above expressions directly into (18), with $\gamma_0 = 2\pi G\rho_0$ we find Dirichlet's result in the following form.

Lemma 4.1. *The linear Lagrangian map in* (14) *provides a solution to the Euler equations if $P(t)$ satisfies*

$$P^T\ddot{P} = \beta(t)I + (\gamma_0 \det\Lambda)S\Lambda\frac{\partial\alpha_0}{\partial\Lambda}S^T, \tag{25}$$

along with the conditions in (16).

Next we want to show how (25) arises from reduced least action, and derive Dedekind's symmetry. Using the fact that $3\int_{B_1} y_i^2\,dy = \frac{4\pi}{5}$, the kinetic energy in (7) is reduced to an expression in terms of $\dot{P}$ via

$$\mathcal{K}(P) = \frac{2\pi}{15}(\rho_0 \det\Lambda_0)\int_0^{\bar{t}} \mathrm{tr}(\dot{P}^T\dot{P})\,dt \tag{26}$$

The gravitational potential energy is reduced to an expression in terms of P via

$$\mathcal{V}(P) = -\frac{1}{2}G(\rho_0 \det\Lambda_0)^2\int_0^{\bar{t}}\int_{B_1^2}\frac{1}{|P(y-y')|}\,dy\,dy'\,dt \tag{27}$$

Note that $\mathrm{tr}(\dot{P}^T\dot{P}) = \mathrm{tr}(\dot{P}\dot{P}^T)$, and since the singular value decomposition of P^T is $S\Lambda R^T$, orthogonal changes of variables in the last integral yields

$$\int_{B_1^2}\frac{1}{|P(y-y')|}\,dy\,dy' = \int_{B_1^2}\frac{1}{|\Lambda(y-y')|}\,dy\,dy' = \int_{B_1^2}\frac{1}{|P^T(y-y')|}\,dy\,dy' \tag{28}$$

By consequence we infer

Lemma 4.2. *The reduced action $\mathcal{A}(P) = \mathcal{K}(P) - \mathcal{V}(P)$ of every matrix path P satisfies*

$$\mathcal{A}(P) = \mathcal{A}(P^T). \tag{29}$$

Since P is a smooth function of P^T and vice versa, the chain rule implies that P^T is a critical path for the (determinant-constrained) action if and only if P is. This is *Dedekind's symmetry*, which he used to discover that Jacobi's rigidly rotating ellipsoids correspond to ellipsoids with steady internal flows.

Lastly, we wish to indicate how the evolution equation (25) arises by least action from the reduced action, due to the orthogonal invariance of the reduced potential energy.

Lemma 4.3. *Given any C^1 function $\mathcal{U} : \mathbb{R}^{m\times n} \to \mathbb{R}$ invariant with respect to both right and left multiplication by orthogonal matrices, its derivative at a matrix P can be expressed in terms of the singular value decomposition $P = R\Lambda S^T$, $\Lambda = \mathrm{diag}\{a_i\}$, in the form*

$$\frac{\partial U}{\partial P} = R\frac{\partial U}{\partial\Lambda}S^T,$$

where

$$\frac{\partial U}{\partial P} = \left(\frac{\partial}{\partial P_{ij}}U(P)\right) \quad \textit{and} \quad \frac{\partial U}{\partial\Lambda} = \mathrm{diag}\left\{\frac{\partial U}{\partial P_{ii}}(\Lambda)\right\}.$$

Proof. By density we may assume the singular values a_i of P are distinct. Then for any perturbation direction $\tilde{P}$ there is a C^1-smooth singular value decomposition

$$P + \varepsilon\tilde{P} = R(\varepsilon)\Lambda(\varepsilon)S(\varepsilon)^T$$

for $|\varepsilon|$ small enough. Letting $'$ denote the derivative in ε, evaluated at $\varepsilon = 0$, we note

$$\Lambda' = R^T \tilde{P} S - R^T R' \Lambda - \Lambda S'^T S$$

Since $\operatorname{tr}(AB) = \operatorname{tr}(BA)$ for any square matrices A and B, we then find by invariance that

$$\begin{aligned}\operatorname{tr}\left(\frac{\partial U}{\partial P}^T \tilde{P}\right) &= \frac{d}{d\varepsilon} U(P + \varepsilon\tilde{P})\Big|_{\varepsilon=0} = \frac{d}{d\varepsilon} U(\Lambda(\varepsilon))\Big|_{\varepsilon=0} = \operatorname{tr}\left(\frac{\partial U}{\partial \Lambda}\Lambda'\right) \\ &= \operatorname{tr}\left(S\frac{\partial U}{\partial \Lambda} R^T \tilde{P}\right) - \operatorname{tr}\left(R^T R' \Lambda \frac{\partial U}{\partial \Lambda}\right) - \operatorname{tr}\left(\frac{\partial U}{\partial \Lambda}\Lambda S'^T S\right) = \operatorname{tr}\left(S\frac{\partial U}{\partial \Lambda} R^T \tilde{P}\right).\end{aligned}$$

The last equality holds because $R^T R'$ and $S'^T S$ are skew while $\Lambda \frac{\partial U}{\partial \Lambda} = \frac{\partial U}{\partial \Lambda}\Lambda$ is symmetric. □

The reduced gravitational potential energy takes a classic expression [35, p. 700] in terms of the singular values a_j of P, using the function $\alpha_0 = \alpha_0(\Lambda)$ from (20), as

$$\mathcal{V}(P) = \frac{1}{2}\rho_0 \int_0^{\bar{t}} \int_{R\Omega_t} \varphi(R\hat{x}, t)\, d\hat{x}\, dt = -\frac{3}{10} G M^2 \int_0^{\bar{t}} \alpha_0(\Lambda(t))\, dt, \qquad M = \rho_0 \frac{4\pi}{3} a_1 a_2 a_3.$$

Therefore the quantity in (28) can be expressed in the form

$$\int_{B_1^2} \frac{1}{|P(y - y')|}\, dy\, dy' = \frac{(4\pi)^2}{15} U(P), \qquad \text{where} \quad U(P) = U(\Lambda) = \alpha_0(\Lambda). \tag{30}$$

Incorporating the constraint $\log\det P(t) = \text{const}$ yields the augmented reduced action

$$\tilde{\mathcal{A}} = \frac{4\pi}{15}\rho_0 \det\Lambda_0 \int_0^{\bar{t}} \left(\frac{1}{2}\operatorname{tr}(\dot{P}^T \dot{P}) + \gamma_0(\det\Lambda_0) U(P) + \beta(t)\log\det P\right) dt$$

Applying Lemma 4.3 after noting $\det P = \det\Lambda$, we find that the criticality condition $\delta\tilde{A} = 0$ subject to the constraint $\det P(t) = \text{const}$ corresponds to the equation

$$\ddot{P} = R\left(\beta(t)\Lambda^{-1} + (\gamma_0 \det\Lambda)\frac{\partial \alpha_0}{\partial \Lambda}\right) S^T, \tag{31}$$

which is equivalent to (25). (It is curious that Lemma 4.3 provides Abel's formula for the derivative of $\log\det P$.)

There is a considerable body of modern literature studying the Hamiltonian dynamics of the reduced dynamics; we refer to Borisov et al. [3], Morrison et al. 2009[47], and Lewis [37] for further discussion and references.

5. Dirichlet ellipsoids and hyperboloids

Next we specialize the discussion to review properties of a family of simple exact solutions to the zero-gravity water wave equations with pressureless free boundaries given by conics. In particular we pay attention to the possible singular features of such flows, focussing on 2D and the development of fluid jets. We remark also upon a geodesic interpretation that proved useful in our study [41] that was motivated by a droplet splitting scenario.

The flows that we study here are all simple straining flows. The ellipsoids are special cases of solutions found by Dirichlet [18], and hyperboloids were found by Longuet-Higgins [42].

5.1. **Geodesic curves of conics.** We now describe some potential flows with conic free surface in any dimension $d \geq 2$. The Lagrangian flow map associated to the velocity field $v = \nabla\phi$ will satisfy

$$\dot{X}(z,t) = \nabla\phi(X(z,t),t), \qquad X(z,0) = z, \tag{32}$$

for all $z \in \Omega_0 \subset \mathbb{R}^d$ and all t. All our flows here will correspond to quadratic potentials of the form

$$\phi(x,t) = \frac{1}{2}\sum_{j=1}^{d} \alpha_j(t) x_j^2 - \lambda(t), \qquad \text{with} \quad \Delta\phi = \sum_{j=1}^{d} \alpha_j(t) = 0, \tag{33}$$

so that the components of the Lagragian map evolve in a purely dilational way according to

$$\dot{X}_j = \alpha_j(t) X_j\,, \quad j = 1,\dots,d. \tag{34}$$

Fixing some $\sigma_0 \in \mathbb{R}$ and some choice of signs $\sigma_j = \pm 1$ for $j = 1,\dots,d$, the fluid will be taken to occupy a domain of the form

$$\Omega_t = \{x \in \mathbb{R}^d : S(x, a(t)) < \sigma_0\}, \tag{35}$$

where we define

$$S(x,a) = \sum_{j=1}^{d} \sigma_j \frac{x_j^2}{a_j^2}\,, \qquad a = (a_1,\dots,a_d) \in \mathbb{R}^d_+\,. \tag{36}$$

The kinematic condition that the boundary flows with the fluid requires that for $z \in \partial\Omega_0$,

$$0 = \frac{1}{2}\frac{d}{dt} S(X,a) = \sum_{j=1}^{d} \sigma_j \frac{X_j^2}{a_j^2}\left(\alpha_j - \frac{\dot{a}_j}{a_j}\right)$$

Leaving degenerate cases aside, it suffices to suppose that

$$\dot{a}_j = \alpha_j a_j\,, \quad j = 1,\dots,d. \tag{37}$$

Due to the incompressibility constraint in (33) it follows that the product

$$a_1 \cdots a_d = r^d \tag{38}$$

remains constant in time.

We recall the simple proof of the following result from [40] (with a slight change of notation) that provides a geodesic interpretation for solutions of the kind considered here.

Proposition 5.1. *Given a constant $r > 0$, let $a(t) = (a_1(t),\dots,a_d(t))$ be any constant-speed geodesic on the surface determined by the relation* (38) *in the space $\mathbb{R}^d_+$ with metric of signature $(\sigma_1,\dots,\sigma_d)$ (possibly indefinite). Then this determines an ideal potential flow with Ω_t as in* (35)*, pressure given by*

$$p(x,t) = \frac{\beta(t)}{2}(\sigma_0 - S(x,a)), \qquad \beta(t) = \frac{\sum_j \dot{a}_j^2/a_j^2}{\sum_j \sigma_j/a_j^2}, \tag{39}$$

and potential ϕ given by (33) *with $\alpha_j = \dot{a}_j/a_j$ and $\dot{\lambda} = \frac{1}{2}\beta\sigma_0$.*

Proof. The path $t \mapsto a(t)$ is a geodesic on the surface defined by (38) with constant squared speed $\sum_j \sigma_j \dot{a}_j^2$ if and only if the acceleration $\ddot{a}$ is parallel to the surface normal. Here this means that there is some scalar $\beta = \beta(t)$,

$$\ddot{a}_j = \frac{\beta\sigma_j}{a_j}, \qquad j = 1,\dots,d. \tag{40}$$

The reason is that such a geodesic is a critical path for the augmented action

$$\tilde{\mathcal{A}} = \int_0^T \sum_j \left(\frac{1}{2}\sigma_j \dot{a}_j^2 + \beta(t) \log \frac{a_j}{r} \right) dt.$$

The value of $\beta(t)$ must be as stated in (39) since we require

$$0 = \frac{d^2}{dt^2} \sum_j \log a_j = \sum_j \frac{a_j \ddot{a}_j - \dot{a}_j^2}{a_j^2}.$$

Define ϕ by (33) with α_j and $\dot{\lambda}$ as stated in the Proposition. Because $\dot{\alpha}_j + \alpha_j^2 = \ddot{a}_j/a_j = \beta\sigma_j/a_j^2$, the pressure from the Bernoulli equation (2) must satisfy

$$p = -\phi_t - \frac{1}{2}|\nabla\phi|^2 = \dot{\lambda} - \frac{1}{2}\sum_j (\dot{\alpha}_j + \alpha_j^2) x_j^2 = \frac{\beta}{2}(\sigma_0 - S(x,a)).$$

Thus $p = 0$ on $\partial\Omega_t$, and the ideal droplet equations all hold. □

Under the present conventions, we note that the Taylor sign condition (4) holds exactly when $p > 0$ in Ω_t, and this occurs exactly when $\beta > 0$ in (39).

5.2. **Ellipsoidal droplets.** The fluid domains Ω_t always remain bounded and ellipsoidal in case $\sigma_j = 1$ for all $j = 0, 1, \ldots, d$. These Dirichlet ellipsoids played an important role in the study of action-infimization for free boundary droplet flows carried out in [41], particularly the ones corresponding to length-minimizing paths.

The solution remains smooth globally for $t \in \mathbb{R}$, since the vector $a(t)$ of semi-major axis lengths moves at a constant (Euclidean) speed $c = |\dot{a}|$ on the surface (38) and cannot reach any singular point in finite time. The pressure $p > 0$ in Ω_t because $\beta > 0$ in (39), so the Taylor sign condition holds, consistent with well-known results on well-posedness for water wave dynamics [59, 60, 38, 15].

Each velocity component $\dot{a}_j$ is increasing, because it turns out that $\ddot{a}_j = \beta\sigma_j/a_j > 0$ for all j. The speed c bounds $|\dot{a}_j|$ for all j as well. As $t \to +\infty$, necessarily some component $a_j \to \infty$, and as $t \to -\infty$, some component $a_k \to \infty$, since $\sum \dot{a}_j/a_j = 0$.

5.3. **Ellipsoidal voids.** The fluid can be considered to occupy the domain *exterior* to the ellipsoids above by taking $\sigma_j = -1$ for all j. In this case, the pressure $p < 0$ in Ω_t because $\beta < 0$ in (39). The Taylor sign condition fails by consequence, and we can expect this 'bubble' flow to be highly unstable.

5.4. **Hyperbolas in 2D.** For the case when the signs of σ_j can differ, the planar case $d = 2$ admits the most simple and complete description. We set $\sigma_0 = \sigma_1 = -1 = -\sigma_2$, so that the domain Ω_t corresponds to

$$\frac{x_1^2}{a_1^2} > 1 + \frac{x_2^2}{a_2^2}. \tag{41}$$

The equations of motion derive solely from incompressibility and geodesic speed constraints:

$$a_1 a_2 = r^2, \qquad -\dot{a}_1^2 + \dot{a}_2^2 = \hat{s} \in \mathbb{R}. \tag{42}$$

Eliminiating $\dot{a}_2$ we find $\dot{a}_1^2(a_2^2 - a_1^2) = \hat{s}a_1^2$, whence with $\tau = \pm\sqrt{|\hat{s}|}$ we have

$$\dot{a}_1 = \frac{\tau}{|\tan^2\theta - 1|^{1/2}}, \qquad \tan\theta = \frac{a_2}{a_1} = \frac{r^2}{a_1^2}. \tag{43}$$

Here $\theta = \theta(t)$ is the angle that the hyperbola's asymptote makes with the x_1 axis.

The pressure from (39) has the same sign as β, which is given here by

$$\beta = \frac{a_2^2\dot{a}_1^2 + a_1^2\dot{a}_2^2}{a_1^2 - a_2^2} = \frac{2\dot{a}_2^2}{1 - \tan^2\theta}.$$

The pressure is positive and the Taylor sign condition (4) holds when $0 < \theta < \pi/4$ ($a_1 > a_2$), and pressure is negative and the Taylor sign condition violated when $\pi/4 < \theta < \pi/2$ ($a_1 < a_2$).

Singularities. No solution exists globally for $t \in \mathbb{R}$. The solution becomes singular in finite time when $a_1 - a_2$ reaches zero, which means that the asymptotic angle θ reaches $\pi/4$. If initially $\theta < \pi/4$ and $\dot{a}_1 < 0$ the solution becomes singular as t increases, but exists globally for $t < 0$ with $a_1 \to \infty$ as $t \to -\infty$. The same happens if $\theta > \pi/4$ and $\dot{a}_1 > 0$. The reverse happens if $\theta < \pi/4$ and $\dot{a}_1 > 0$, or if $\theta > \pi/4$ and $\dot{a}_1 < 0$—the solution exists globally for $t > 0$ with $a_1 \to \infty$ as $t \to +\infty$.

In all cases, the *free surface shape remains smooth* approaching a singular time. If the Taylor sign condition holds and t increases approaching singularity, the angle between the asymptotes widens and approaches 90°. The pressure and fluid velocity blow up *everywhere*, since $\alpha_1 = \dot{a}_1/a_1$ blows up. Of course, the domain is unbounded and the energy is infinite, so it is unclear whether this is relevant for any finite energy flow.

Corners. No free-surface singularity occurs in any solution we have discussed so far. As Longuet-Higgins [44] pointed out, one obtains a simple flow containing a corner for all time, in a limit obtained by "zooming out." Here it corresponds to taking $\sigma_0 = 0$, so that for example Ω_t corresponds to the sector of the plane where

$$\frac{x_1}{a_1(t)} > \frac{|x_2|}{a_2(t)}$$

The same equations (42) and (43) govern the evolution of the sector opening angle. As above, the Taylor sign condition holds if the corner angle 2θ is less than 90° and is violated if it is greater than 90°. Blowup occurs in the same ways as before.

The condition $2\theta < 90°$ is consistent with the theory for water waves with persistent corners developed by Kinsey and Wu [34] and Wu [61], since corners with angles less than 90° have the finite "energy" defined in [34] necessary to apply their theory.

6. Locally singular ballistic interfaces

Recently, Zubarev and Karabut [66] and Zhuravleva et al. [65] have described rather explicit examples of ideal fluid flows on unbounded fluid domains that are capable of developing local singularities on the free surface. These examples provide solutions of the ideal droplet equations (1)–(3) that are derived from particular holomorphic solutions of the complex Hopf equation or inviscid Burgers equation

$$V_t + VV_z = 0 \quad \text{for } z \in \Omega_t. \tag{44}$$

Here $z = x + iy \in \Omega_t \subset \mathbb{C}$ corresponds to Eulerian variables in the fluid domain.

A solution of (44) corresponds to a solution of (1)–(3) via

$$V = u - iv = \phi_x - i\phi_y\,, \tag{45}$$

provided (i) V is holomorphic in z on Ω_t (ii) the pressure-velocity relation

$$p = -v^2 \quad \text{in } \Omega_t \tag{46}$$

holds, and (iii) the pressure vanishes on $\partial\Omega_t$, i.e., (3) holds. This last condition means that fluid particles on the boundary move purely horizontally, and indeed the boundary must

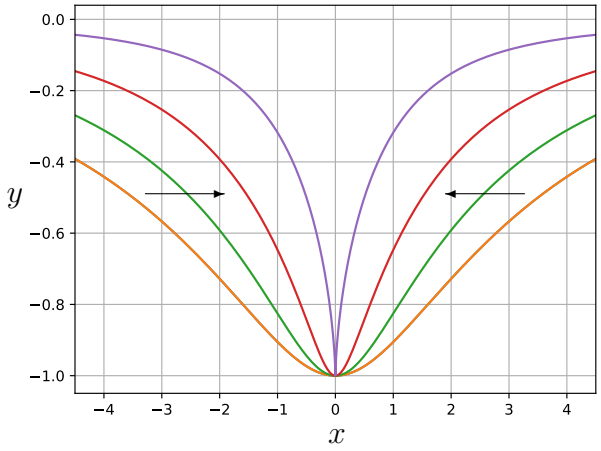

FIGURE 1. The interface in (49) for $t = -4, -3, -2, -1$ (from bottom to top)

satisfy

$$\operatorname{Im} V = 0 \quad \text{on } \partial\Omega_t. \tag{47}$$

As one can verify by straightforward computation, the real and imaginary parts of the Hopf equation yield Euler's equations, noting $p_x = -2vu_y$, $p_y = -2vv_y$.

The characteristic curves $Z(t)$ for the Hopf equation are straight lines that satisfy

$$\frac{dZ}{dt} = V(Z(t), t), \qquad \frac{d}{dt}V(Z(t), t) = 0.$$

When $v \neq 0$, these curves are not fluid particle paths. However, *on the free surface where $p = 0$ they are particle paths.* Consequently, particle paths on the surface evolve *in straight lines, horizontally at constant speed.*

In [66], the authors find solutions by solving implicitly characteristic equations in the form

$$z = Vt + F(V). \tag{48}$$

Here $F(V) \to 0$ as $V \to \infty$ for the values of V relevant to the solution, and F should be chosen to avoid singularities when z is in the fluid domain. The case $F(V) = 1/(V + i)$ is the simplest one that provides local singularities. In this case one can use the horizontal velocity u to parametrize the free surface via

$$z = tu + \frac{1}{u + i} = tu + \frac{u}{u^2 + 1} - \frac{i}{u^2 + 1}, \quad u \in \mathbb{R}. \tag{49}$$

We plot this surface for $t = -4, -3, -2, -1$ in Fig. 1. The surface is a smooth graph $y = \gamma(x, t)$ for $t < -1$, since $dx/du < 0$ for all u. A cusp develops at $t = -1$, having $y \sim -1 + |x|^{2/3}$.

Very recently, Zhuravleva et al. [65] have described a different family of solutions of the ideal droplet equations that describe unbounded flows surrounding a collapsing cavity. They use holomorphic solutions to the complex Hopf equation (44) to determine fluid velocity in a different way, namely

$$u - iv = \frac{1}{V}, \tag{50}$$

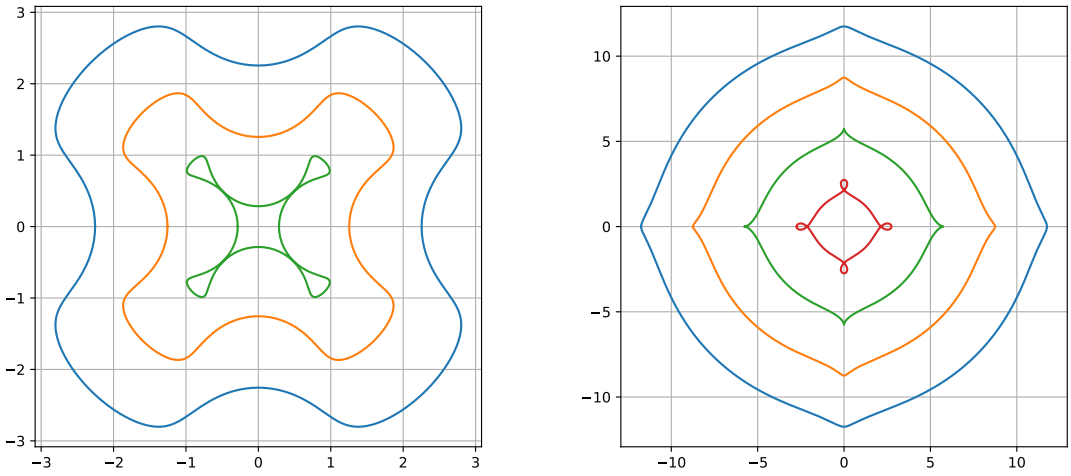

FIGURE 2. Collapsing cavity with splash and local singularities.
(Left: $a = -0.2$, $t = -3, -2, -1.03$. Right: $a = 0.2$, $t = -11, -8, -5, -2$.)

and impose a different pressure-velocity relation, namely

$$p = \frac{1}{2}\log(u^2 + v^2) - \frac{u^2 + v^2}{2} + \frac{1}{2} \tag{51}$$

On the fluid boundary in this case, vanishing pressure necessitates the condition

$$|V| = 1 \quad \text{for } z \in \partial\Omega_t. \tag{52}$$

Then on the free surface, one finds ballistic particle paths that coincide with characteristics according to the relations

$$z = (u + iv)t + z_0 = Vt + G(V)\,. \tag{53}$$

The fluid interface can be determined parametrically by using (48) with the relation $V = e^{i\theta}$ on the fluid boundary. Corresponding to the choice

$$G(V) = \frac{4aV}{1 - b^4V^4}, \quad a = -0.2, \quad b = 1.2, \tag{54}$$

the authors in [65] show that the cavity collapses to a splash singularity, as shown in the left panel of Fig. 2, where the interface is shown at times $t = -3, -2, -1.03$ as in [65]. In the right panel, we take $a = 0.2$ instead and plot at the times $t = -11, -8, -5, -2$. The figure indicates that a local singularity forms at a time $t \approx -5$ and loses physical meaning after a self-intersection appears. Indeed, a local singularity must appear at the time $t = -G'(1) \approx -5.01176$ when the boundary parametrization degenerates. (For sufficiently large negative times, $\partial z/\partial V \neq 0$ for $|V| = 1$ and injectivity of the map $V \mapsto z$ for $|V| < 1$ follows by classical criteria, see section A.5 below.)

For all of the singular solutions found in [66] and [65], the fluid particles on the free surface experience zero acceleration. Indeed, the gradient of the pressure vanishes at the free surface

in each of the respective cases (46) and (51). By consequence we have

$$\frac{\partial p}{\partial n} = 0 \quad \text{on } \partial\Omega_t, \tag{55}$$

so the strict Taylor sign condition (4) does not hold. Necessarily, $p < 0$ inside the fluid domain, in fact, for both cases (46) and (51).

While the solutions in [66] are certainly interesting, then, it seems difficult to imagine how they might approximate solutions of (1)–(3) in bounded domains, since for the latter, $-p$ is always subharmonic due to (2), so $p > 0$ in the fluid domain.

7. Numerical evidence for 2D local singularities

In this section our goal is to study the possible development of local singularities in smooth ideal potential flows through the use of several numerical illustrations and experiments.

Initially we expected that with zero gravity and surface tension, corners in the free surface would form rather easily, as the fluid 'tries to move ballistically' except for the pressure term that maintains incompressibility. As illustrated in the first examples below, however, our experience is consistent with the observations and remarks of Longuet-Higgens [45], who used three-dimensional Dirichlet hyperboloids to explain jets in several kinds of fluid experiments, and argued that such hyperboloidal jets may be characteristic of other types of unsteady free-surface flows.

As we illustrated in [40], it is not difficult to find and compute flows that exhibit a splash singularity, with interface that self-intersects at some positive time. By varying parameters, we attempted to find flows with local singularities forming as self-intersection points merge together. But instead we found a tendency for strongly curved interfaces to be unstable through the formation of small-scale (presumably hyperbolic) jets.

In [40], this led us to consider the expedient of exploiting the time-reversal symmetry of the Euler equations. We computed solutions *expanding away* from a corner. Starting with a sequence of smooth approximations to a nonsmooth fluid domain, our computations suggested convergence to a smooth interface with bounded curvature at positive time.

In the last subsection below, we extend these computations using equations (62) instead of (58), and with different initial data. The results are consistent with the previous ones in [40], and are suggestive of a self-similar scaling hypothesis for a two-parameter family of smooth solutions starting from an interface formed by an infinite wedge with power-law initial velocity. We also provide a heuristic explanation of the scaling exponents that are observed here and were first seen in [40].

7.1. **Conformal formulations and a pseudospectral scheme.**

We perform our computations using a filtered pseudospectral discretization of the equations of motion in a conformal formulation. An advantage of this approach that is well known is that the Dirichlet-to-Neumann map for the fluid domain is replaced by that for the reference domain, which is easier to compute.

For the case that we study here, we will take the reference domain to be the unit disk $\mathbb{D} \subset \mathbb{C}$. With this choice we can make use of the Möbius automorphisms of $\mathbb{D}$ to concentrate grid points in some zone of high curvature. An analogous transformation for periodic water waves was described in [46]. This method is convenient, but is limited in its capability to resolve fine-scale flow features, as compared to more flexible boundary integral methods with adaptive grid refinement, say.

Formulations. We refer to the appendix for a detailed derivation of the two conformal formulations that we make use of. Briefly, we let $z = x + iy$ denote complexified Eulerian

coordinates in the fluid domain $\Omega_t \subset \mathbb{C}$. This domain is assumed to be parametrized by a conformal map $w \mapsto \mathbf{Z}(w,t)$, $w \in \mathbb{D}$. The boundary $\partial\Omega_t$ is then parametrized by $\theta \in \mathbb{T} = \mathbb{R}/2\pi\mathbb{Z}$ via

$$z = Z(\theta,t) := \mathbf{Z}(e^{i\theta},t), \quad \theta \in \mathbb{T}.$$

Since $Z = X + iY$ provides the boundary values of a holomorphic function in $\mathbb{D}$, the real part determines the imaginary part by the Hilbert transform. With the expansion

$$Z = \sum_{k\in\mathbb{Z}} \hat{Z}_k(t) e^{ik\theta}, \quad Z_k = X_k + iY_k, \tag{56}$$

we have (presuming $\hat{Y}(0,t) = 0$ for convenience)

$$Y = HX, \quad \text{meaning} \quad \hat{Y}_k(t) = (-i \operatorname{sgn} k)\hat{X}_k(t).$$

The first conformal formulation involves $\boldsymbol{Z}(w,t)$, the conformal parametrization of the fluid domain, and $\boldsymbol{F}(w,t)$, the complex velocity potential. Under the simplest conditions that uniquely fix the fluid parametrization, which are

$$\frac{d}{dt}\boldsymbol{Z}(0,t) = 0, \qquad \frac{d}{dt}\arg \boldsymbol{Z}_w(0,t) = 0, \tag{57}$$

the evolution equations for these quantities take the following form:

$$\boldsymbol{Z}_t = \boldsymbol{Z}_w \boldsymbol{G}, \qquad \boldsymbol{F}_t = \boldsymbol{F}_w \boldsymbol{G} - \boldsymbol{R}, \tag{58}$$

where the traces G, R of the holomorphic functions $\boldsymbol{G}, \boldsymbol{R}$ are respectively given by

$$G = w(I + iH)\operatorname{Re}\left(\frac{U}{n}\right), \qquad R = (I + iH)\left(\frac{1}{2}|U|^2\right). \tag{59}$$

Here surface pressure and body forces have been taken as zero. In these expressions, U and n are the traces of the (anti-holomorphic) velocity $\boldsymbol{U}$ and (unnormalized) normal vector $\boldsymbol{n}$, given by

$$\bar{\boldsymbol{U}} = \frac{\boldsymbol{F}_w}{\boldsymbol{Z}_w}, \qquad \boldsymbol{n} = w\boldsymbol{Z}_w. \tag{60}$$

We make use of a second conformal formulation in order to study dynamics in a very large domain approximating an infinite wedge. The holomorphic function

$$\boldsymbol{Q} = \frac{1}{\boldsymbol{Z}_w}, \tag{61}$$

evolves together with $\bar{\boldsymbol{U}}$ according to the equations

$$\boldsymbol{Q}_t = \boldsymbol{Q}_w \boldsymbol{G} - \boldsymbol{Q}\boldsymbol{G}_w\,, \qquad \bar{\boldsymbol{U}}_t = \bar{\boldsymbol{U}}_w \boldsymbol{G} - \boldsymbol{Q}\boldsymbol{R}_w\,, \tag{62}$$

with the traces of $\boldsymbol{G}$ and $\boldsymbol{R}$ given as in (59). Essentially this same formulation was described by A. I. Dyachenko in [20] and was used recently by S. A. Dyachenko [23] to compute bounded ideal droplet solutions with and without surface tension.

In each of the two formulations, we compute by evolving just the real parts of the traces and determining the imaginary parts using the Hilbert transform. To recover the boundary parametrization Z from the second formulation in a nonsingular way for large domains not encircling 0, it is sometimes convenient to write

$$\boldsymbol{S} = \frac{1}{\boldsymbol{Z}} \tag{63}$$

(or some other analytic function of $1/\boldsymbol{Z}$) and evolve $\boldsymbol{S}$ (actually the real part of its trace) along with (62) according to

$$\boldsymbol{S}_t = \boldsymbol{S}_w \boldsymbol{G}\,. \tag{64}$$

When $1/\boldsymbol{Q}$ is not singular, we recover Z by integrating with respect to w using the fast Fourier transform as indicated below.

Verification of (62). For completeness we derive (62) from (58). Since $\bar{\boldsymbol{U}} = \boldsymbol{Q}\boldsymbol{F}_w$, we get

$$\boldsymbol{Q}_w = -\boldsymbol{Q}^2\boldsymbol{Z}_{ww}\,, \qquad \bar{\boldsymbol{U}}_w = \boldsymbol{Q}\boldsymbol{F}_{ww} + \boldsymbol{Q}_w\boldsymbol{F}_w\,,$$

$$\boldsymbol{Z}_{wt} = \boldsymbol{Z}_{ww}\boldsymbol{G} + \boldsymbol{Z}_w\boldsymbol{G}_w\,, \qquad \boldsymbol{F}_{wt} = \boldsymbol{F}_{ww}\boldsymbol{G} + \boldsymbol{F}_w\boldsymbol{G}_w - \boldsymbol{R}_w\,.$$

Then it follows $\boldsymbol{Q}_t = -\boldsymbol{Q}^2\boldsymbol{Z}_{wt} = \boldsymbol{Q}_w\boldsymbol{G} - \boldsymbol{Q}\boldsymbol{G}_w$ and $\bar{\boldsymbol{U}}_t = \boldsymbol{Q}_t\boldsymbol{F}_w + \boldsymbol{Q}\boldsymbol{F}_{wt}$, so

$$\bar{\boldsymbol{U}}_t = (\boldsymbol{Q}_w\boldsymbol{G} - \boldsymbol{Q}\boldsymbol{G}_w)\boldsymbol{F}_w + \boldsymbol{Q}(\boldsymbol{F}_{ww}\boldsymbol{G} + \boldsymbol{F}_w\boldsymbol{G}_w - \boldsymbol{R}_w) = \bar{\boldsymbol{U}}_w\boldsymbol{G} - \boldsymbol{Q}\boldsymbol{R}_w\,.$$

Discretization. We use a straightforward psuedospectral scheme to discretize the equations in space, using grid points $\theta_j = jh$, $j = 1, \ldots, N$, $h = 2\pi/N$. For the system (58), we first expressed the equations in real form in terms of the operator $\partial_\theta = iw\partial_w$, and then filter all derivatives by replacing ∂_θ with Fourier symbol ik by $\mathcal{D}_\rho$ with Fourier symbol

$$\hat{\mathcal{D}}_\rho(k) = ik\,\rho(hk), \qquad \rho(\xi) = \exp(-10(\xi/\pi)^{15})$$

This filter is similar to that used in [27]. We use a standard ODE solver in the julia OrdinaryDiffEq package for time integration, with tolerance set to 10^{-9} or smaller.

For system (62) we convert real parts to complex analytic form by the discrete Hilbert transform, e.g., representing $Q(\theta_j, t)$, $j = 1, \ldots, N$ by

$$Q_j(t) = \sum_{k=0}^{N/2-1} \hat{Q}_k(t) e^{ik\theta_j}\,, \tag{65}$$

then compute filtered derivatives by using the fast Fourier transform to evaluate

$$(\mathcal{D}_\rho Q)_j = \sum_{k=1}^{N/2-1} ik\rho(hk) Q_k e^{i(k-1)\theta_j}. \tag{66}$$

We sometimes found it useful for numerical stability to additionally filter the solution after each time step. We recover the interface position when $1/Q$ is nonsingular using the formula

$$Z_j(t) = \sum_{k=1}^{N/2-1} \frac{c_{k-1}(t)}{k} e^{ik\theta_j}\,, \tag{67}$$

assuming $\boldsymbol{Z}(0,t) = 0$, where the coefficients $\hat{c}_k(t)$ are the discrete Fourier coefficients of $1/Q$.

Accuracy check. We checked the accuracy of the numerical scheme for a Dirichlet ellipse as described in section 5.2 above, with initial data for (58) given by

$$Z(\theta, 0) = e^{i\theta}, \qquad F(\theta, 0) = e^{2i\theta}. \tag{68}$$

This corresponds to $a_1(0) = a_2(0) = 1$ in (35) and $\alpha_1(0) = 1$, $\lambda(0) = 0$ in (33). To check how closely the solution conforms to an ellipse, we use an explicit conformal map from ellipse to disk given by

$$z = x + iy \mapsto w = \mathcal{W}_q(z) := \sqrt{k(q)}\,\mathrm{sn}\left(\frac{2K}{\pi}\sin^{-1} z; q\right), \quad q = \left(\frac{a-b}{a+b}\right)^2. \tag{69}$$

Here sn is the Jacobi elliptic function with parameters q, $k(q)$, and $K = K(q)$, with notation as in [48, p. 296]. To evaluate this function, we ported the Matlab routine ELLIPJI by I.

N	E_{ZF}	E_{QU}
64	7.945e-4	9.475e-4
128	8.078e-6	8.315e-6
256	8.576e-9	3.175e-9
512	1.342e-12	2.057e-13
1024	1.898e-11	3.096e-14

TABLE 1. Maximum-norm position errors for elliptical test case at $t = 0.25$

Moiseev [29] to julia. For each system (58) and (62), we tabulate in Table 1 the maximum pointwise error $E = E_{ZF}$ or E_{QU} respectively, given by

$$E = \max_j |\mathcal{W}_q(Z_j) - e^{i\theta_j}|$$

at time $t = 0.25$, assuming the value $a = \frac{1}{b} \approx 1.278$ in (69) is given by $\operatorname{Re} Z_j(t)$ with $j = 0$ from the computed solution. We specified a tolerance of 10^{-12} to the ODE solver for these computations.

7.2. **Examples with developing jets.**

7.2.1. *Initial velocity with five-fold symmetry.* In our first example we take the initial shape as a circle, with five-fold symmetric initial velocity, corresponding to

$$\boldsymbol{Z}(w,0) = w, \quad F(w,0) = -0.15w^5, \quad \boldsymbol{Q}(w,0) = 1, \quad \bar{\boldsymbol{U}}(w,0) = -0.75w^4.$$

We computed the solution from (62) with $N = 2^{14}$ grid points and plot the solution along with a quiver plot of velocity, at time $t = 0.3$ in Fig. 3, The interface shows the development of regions of high curvature that may be incipient jets or corners. The arrows, which are plotted at consecutive grid points, indicate that the uniformly spaced grid on the parametrizing circle is being stretched severely as the jets develop.

7.2.2. *Initial velocity with single mode.* To study whether the protruberances that develop in the previous example might develop into corners, in [40] we considered an initial velocity that produces a single tip. This allows us to use a Möbius transformation to concentrate grid points in the single region of high curvature and resolve the computation for a longer time. Thus we solve equations (58) with initial data satisfying

$$\mathbf{Z}(w,0) = \zeta_r(w) := \frac{w+r}{1+rw}, \qquad \operatorname{Re} F(w,0) = \left(\frac{\operatorname{Re}\mathbf{Z}(w,0)+1}{2}\right)^5. \tag{70}$$

Corresponding to compressing the grid by the factor

$$c = \left(\frac{1+r}{1-r}\right)^2 = 250, \tag{71}$$

we take $r \approx 0.881$. Figure 4, taken from [40], shows the interface computed at time $t = 0.6$ with $N = 1024$ points, compared with a hyperbola of the form

$$\frac{(x-x_0)^2}{a^2} + \frac{y^2}{b^2} = 1, \quad a = 0.532, \quad b = .199, \quad x_0 = 2.398. \tag{72}$$

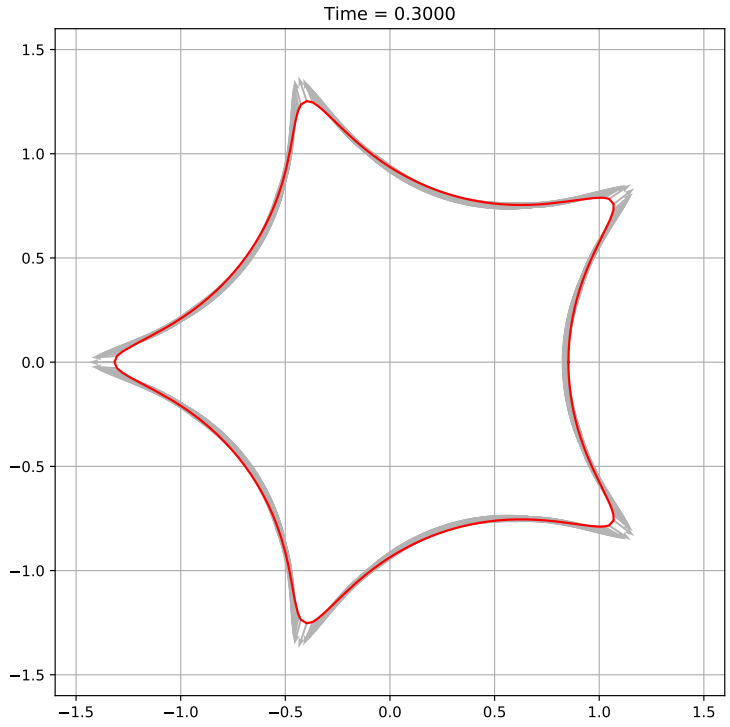

FIGURE 3. Interface from five-fold symmetric initial velocity

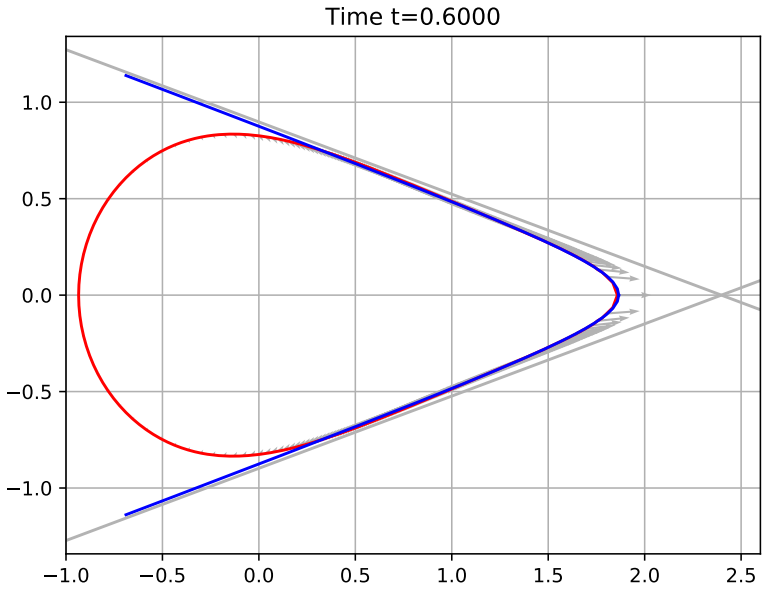

FIGURE 4. Single-mode initial velocity with fit to hyperbola

This hyperbola was found using the polyfit function in julia by fitting 150 values of Y^2 to a quadratic function of X.

The excellent fit of the hyperbola to the "Pinocchio-like nose" developing from the fluid domain suggests that no singularity will ever form as time increases. Rather the nose should grow without bound, with decreasing angle between the asymptotes of the hyperbola, like Longuet-Higgens' exact Dirichlet hyperbola solutions that we described in section 5.

7.3. **A scenario for corner formation.**

7.3.1. *Initial data.* As discussed earlier, we seek to approximate a smooth flow expanding away from a sharp corner. To do so, we will specify an initial interface that is a smooth approximation to a wedge-shaped domain Ω_Θ with opening angle $\Theta \in (0,\pi)$ (as measured outside the fluid domain). The wedge domain can be parametrized by the unit disk $\mathbb{D}$ by composing the map defined by

$$\zeta_\Theta(w) := w^\nu, \qquad \nu = 2 - \frac{\Theta}{\pi} \in (1,2), \tag{73}$$

that takes the right half plane $\operatorname{Re} w > 0$ onto Ω_Θ, with a map

$$\zeta_+(w) = C_+ \left(-1 + \frac{2}{1-w}\right), \quad C_+ > 0, \tag{74}$$

that takes the unit disk onto the right half plane.

To fashion a smooth, bounded approximation to this infinite, singular domain, we use a map that takes the unit disk slightly inside itself, creating a small 'dimple' (with an approximately Gaussian shape) near the point $w = -1$, according to the prescription

$$\zeta_d(w) = w \exp\left(-(I + iH)\left(\varepsilon_1 \cos^{\nu_1}\frac{\vartheta}{2} + \varepsilon_2 \cos^{\nu_2}\vartheta\right)\right), \quad \vartheta = \arg(-w),$$

where we take $\varepsilon_1 = 0.1$, $\nu_1 = 81$, $\varepsilon_2 = 10^{-5}$, $\nu_2 = 20\nu_1$. Finally, the initial interface at time $t_0 = 1$ is determined by the composition

$$\boldsymbol{Z}(w, t_0) = \zeta_\Theta \circ \zeta_+ \circ \zeta_d \circ \zeta_r(w), \tag{75}$$

where the first map ζ_r is the Möbius automorphism of the disk $\mathbb{D}$ from (70) and is used to concentrate points on one side of the circle, and we take $C_+ = 2/\varepsilon_1$ which results in $\boldsymbol{Z}(-1, t_0) \approx 1$.

For the wedge domain, a holomorphic velocity potential $f_\Theta(z) = z^\alpha$ determines a velocity field (u, v) via

$$u - iv = f_\Theta'(z) = \alpha z^{\alpha-1}. \tag{76}$$

We use this velocity formula to determine initial data for the parametrized domain via

$$\bar{\boldsymbol{U}}(w, t_0) = f_\Theta' \circ \boldsymbol{Z}(w, t_0).$$

On the wedge boundary where $z \in \partial\Omega_\Theta$, we have $\arg z = \frac{\pi}{2}\nu$ and $\arg(u + iv) = (1-\alpha)\arg z$. If we make the choice (as was always done in [40])

$$\alpha = \frac{1}{\nu}, \tag{77}$$

then $\alpha \arg z = \frac{\pi}{2}$ and the velocity is normal to the wedge boundary. Below we exhibit examples both with and without this choice, corresponding to the two cases $\alpha\nu = 1$ and $\alpha\nu = \frac{3}{4}$.

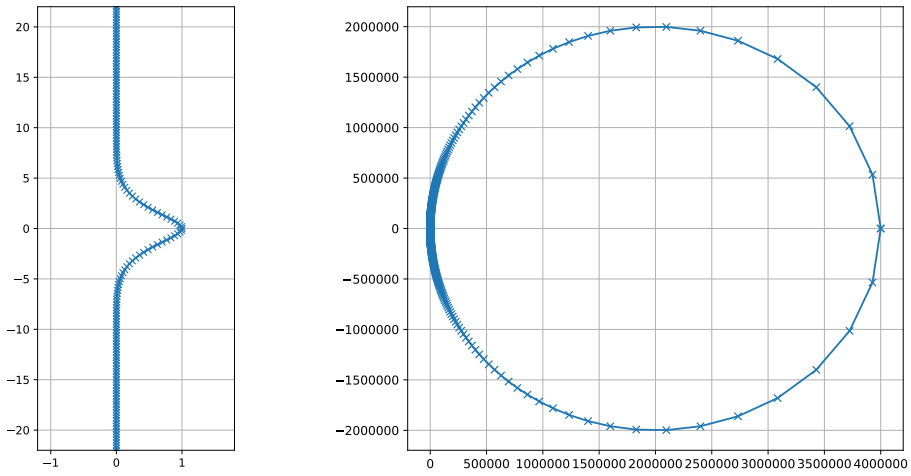

FIGURE 5. The interface $Z(\theta, t_0)$ for $\nu = 1$, $N = 2^{15}$

Parameters. For all the computations reported here, we discretize $\theta \in [0, 2\pi)$ using $N = 2^{15}$ points. We take the grid compression ratio in (71) to be $c = 20000$ in the case $\alpha\nu = 1$, and $c = 4000$ in the case $\alpha\nu = \frac{3}{4}$, and determine r accordingly.

In Fig. 5 we illustrate the effect of the regularizing map ζ_d by taking $\nu = 1$ and plotting $Z(\theta, t_0) = \boldsymbol{Z}(e^{i\theta}, t_0)$. The left panel indicates there is a large region around 0 where the interface is very close to flat, aside from a roughly Gaussian-shaped depression. The right panel shows how the behavior of the interface near infinity is regularized by the factor in ζ_d with ε_2, yielding $\boldsymbol{Z}(1, t_0) \approx 4/(\varepsilon_1\varepsilon_2) = 4 \times 10^6$.

In Fig. 6 we plot $-X$ vs Y and corresponding velocity for the initial interface in the case $\Theta = 60°$, $\nu = \frac{5}{3}$, $\alpha\nu = \frac{3}{4}$. In this orientation, 'water' is below 'air' in the zoomed-in left panel. The arrows inidicate the initial velocity in the case $\alpha\nu = 1$, but we use the same initial interface also in the case $\alpha\nu = \frac{3}{4}$.

7.3.2. *Time evolution.* The computations reported here are carried out using the (less singular) variables $\boldsymbol{Q} = 1/\boldsymbol{Z}_w$, $\boldsymbol{V} = \bar{\boldsymbol{U}}$ and $\boldsymbol{S} = \boldsymbol{Z}^{-1/\nu}$ satisfying equations (62) and (64). The results are generally consistent with those reported in [40] which were performed using equations (58) on somewhat less singular domains. E.g., Fig. 6 indicates that at the initial time $t_0 = 1$, $\boldsymbol{Z}(1, t_0) \approx 10^{10}$ whereas this was $\approx 10^3$ for the case $\Theta = 90°$ considered in [40].

As shown in Fig. 7 (for $\alpha\nu = 1$) and in Fig. 8 (for $\alpha\nu = 0.75$), the interface expands away from the origin and the curvature decreases by a large factor. Upon rescaling as described with small ε as described above, this is consistent with the possible development of an interface with an initial tiny radius of curvature to one with radius of curvature hundreds or thousands of times larger.

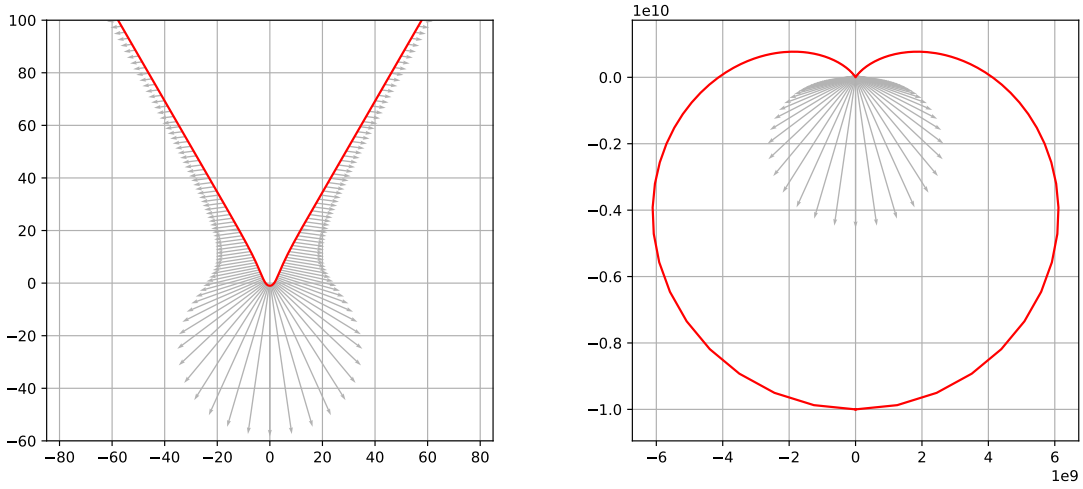

FIGURE 6. Initial interface for $\Theta = 60°$ and velocity for $\alpha = \frac{9}{20}$ in 'water' orientation

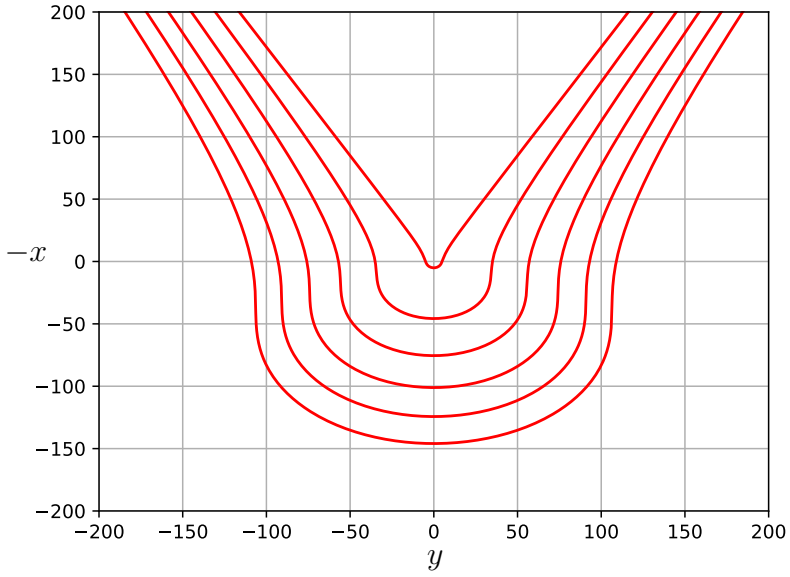

FIGURE 7. Interface for $t = 10$ and $200n$ for $1 \le n \le 5$, with $\Theta = 60°$, $\alpha = \frac{3}{5}$.

7.3.3. *Evidence for self-similarity.* We emphasize here that the Euler equations here are invariant under scaling time and space by the same factor. Thus, although we take $\boldsymbol{Z}(-1, 1) \approx 1$ in our computations, this corresponds to another solution with $\boldsymbol{Z}(-1, \varepsilon) \approx \varepsilon$ for any $\varepsilon > 0$.

The numerical results above and in [40] lead us to expect a power-law scaling in time with $\boldsymbol{Z}(-1, t) \sim ct^{\beta}$ for some $c, \beta > 0$. In Figs. 9 and 10 we plot the *reciprocals* of time-scaled

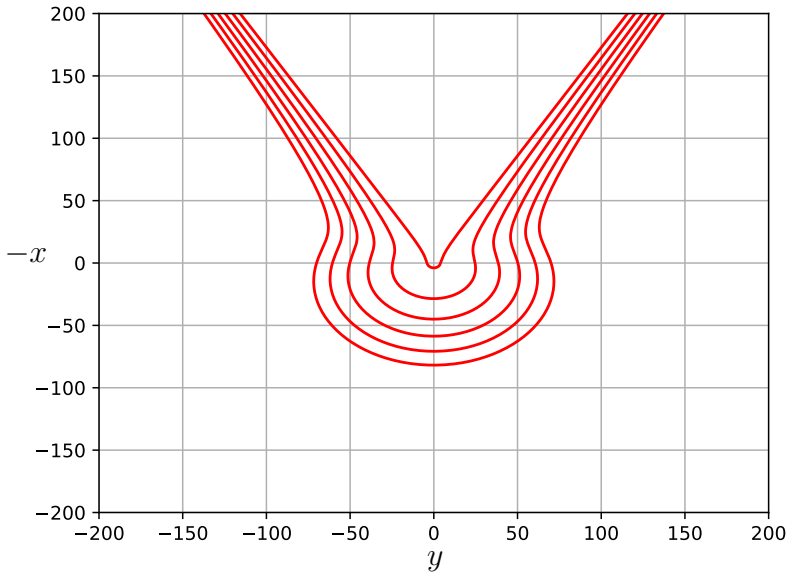

FIGURE 8. Interface for $t = 10$ and $200n$ for $1 \le n \le 5$, with $\Theta = 60°$, $\alpha = \frac{9}{20}$.

interfaces in the water orientation, for the choice (explained below)

$$\beta = \frac{1}{2-\alpha}\,. \tag{78}$$

For $\alpha = \frac{1}{\nu} = \frac{3}{5}$ this yields $\beta = \frac{5}{7}$, and for $\alpha = \frac{3}{4\nu}$ we get $\beta = \frac{20}{31}$. Precisely, we plot

$$\frac{-it^\beta}{Z(\theta,t)} \tag{79}$$

at a sequence of times $t = t_n$ for $n = 1, 2, \dots 10$ ($t_n = 500n$ for $\alpha\nu = 1$, $t_n = 1000n$ for $\alpha\nu = \frac{3}{4}$). These plots allows one to visualize the entire inverted fluid domain, with the origin of the plot corresponding to the fluid far field.

The plots demonstrate a very tight collapse, with the zoomed-in view suggesting convergence to an invariant limit shape. By the scaling invariance argument mentioned above, this result suggests the possible existence of a self-similar solution starting at time $t = 0$ from the exact wedge Ω_Θ with initial power-law potential $f_\Theta(z) = z^\alpha$.

7.3.4. *Scaling argument.* We can provide a two-step heuristic argument to explain the scaling exponent β in (78). Motivated by the results above, it is natural to seek a self-similar solution to the governing equations (1)–(3) by scaling the space variables and potential according to

$$(x, y) = (t^\beta \tilde{x}, t^\beta \tilde{y}), \qquad \phi(x, y, t) = t^\gamma \tilde{\phi}(\tilde{x}, \tilde{y})\,. \tag{80}$$

Simple substitution shows that the linear terms in the Bernoulli equation (2) can balance with the nonlinear terms on the boundary only if

$$\gamma = 2\beta - 1\,. \tag{81}$$

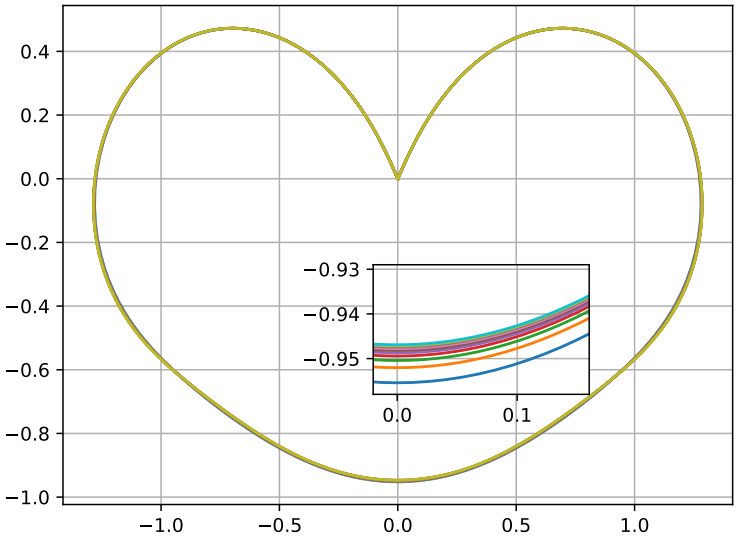

FIGURE 9. Scaled inverse interfaces at $t = 500n$, $1 \le n \le 10$, $\Theta = 60°$, $\alpha = \frac{3}{5}$

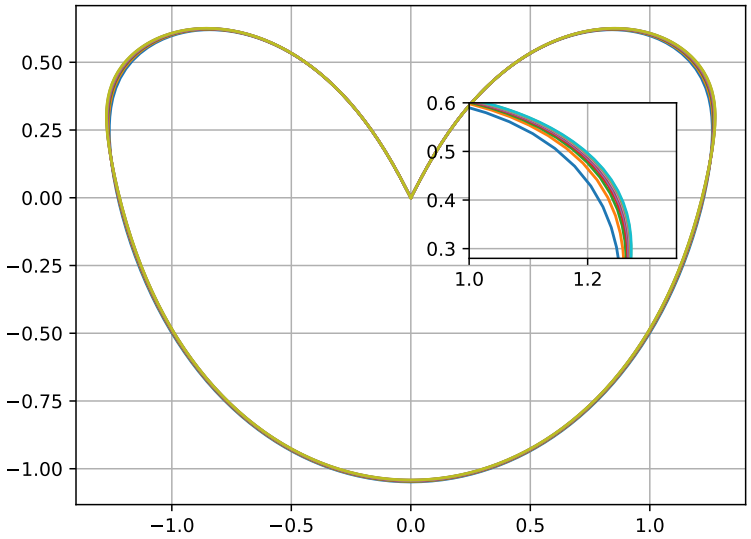

FIGURE 10. Scaled inverse interfaces at $t = 1000n$, $1 \le n \le 10$, $\Theta = 60°$, $\alpha = \frac{9}{20}$

This is the first step. In the second step, writing $\tilde{\phi} = \operatorname{Re} \tilde{f}(\tilde{z})$ with $\tilde{z} = \tilde{x} + i\tilde{y}$, we find that the initial data requirement in (76) as $t \downarrow 0$ imposes the limit relation

$$u - iv = t^{\gamma-\beta} \tilde{f}'(t^{-\beta} z) \to \alpha z^{\alpha-1} \tag{82}$$

when taking $t \downarrow 0$ with $z = x + iy$ fixed. Thus we can expect that

$$\tilde{f}'(\tilde{z}) \sim \alpha \tilde{z}^{\alpha-1} \quad \text{as } \tilde{z} = t^{-\beta} z \to \infty,$$

which entails the relation

$$\gamma = \alpha\beta. \tag{83}$$

Putting (83) together with (81) yields (78).

8. Discussion

Our experience in computing protruberances that emerge from the main body of fluid is consistent with the observations and suggestions of Longuet-Higgens, who pointed out that such protrusions may often take the form of Dirichlet hyperboloids. Such hyperboloidal jets exist with narrowing "nose" that persist and remain smooth forever, despite lacking any regularizing effect from surface tension, viscosity, or gravity. Thus ideal droplets with smooth boundary do not seem to readily form local singularities, consistent with the analytical constraints provided in the work of Kinsey and Wu [34] and Wu [61].

However, our computations presented in section 7.3 strongly suggest that corner formation may occur in an unstable manner for specially prepared initial data in bounded domains. After time-reversal, it appears that a smooth interface may emerge from initial data containing a corner.

"Zooming in," it appears plausible that a corner can form in an asymptotically self-similar way, with a rather general exterior angle and power-law velocity profile approaching the corner. Thus we conjecture that a two-parameter family of self-similar solutions of the ideal droplet equations may exist in infinite, asymptotically wedge-shaped domains. Determining whether such solutions do indeed exist appears to be a difficult challenge for analysis. We point out that if such solutions exist with x-intercept proportional to t^β, then the acceleration of the interface at this point would blow up strongly, like $t^{\beta-2}$.

Acknowledgements

The authors are grateful to Sergey Gavriluk for historical references regarding ellipsoidal solutions. This material is based upon work supported by the National Science Foundation under grants DMS 1812673 and DMS 2106988 (JGL) and grants DMS 1812609 and DMS 2106534 (RLP).

Appendix A. Conformal mapping formulation and least action principles

For water wave equations with gravity, conformal mapping formulations of time dependent flows were described and employed for purposes of analysis by, for example, Ovsjannikov [49], Kano & Nishida [31], and Wu [59], and recently by Hunter et al. [28]. For purposes of numerics and formal analysis such conformal formulations were described by Dyachenko *et al.* [21], Chalikov and Sheinin [10], Choi and Camassa [12], and were extensively developed recently in [24, 22, 46].

Our aim in this appendix is to provide a pedagogical derivation of the ideal droplet equations in terms of a time-dependent conformal mapping of the disk $\mathbb{D}$ onto the fluid domain Ω_t, especially taking into account the freedom of choice in parametrization afforded by the automorphism group of $\mathbb{D}$. Using a special, simple choice that fixes one point of the map from $\mathbb{D}$ to Ω_t, a conformal mapping formulation for droplets was written already by Ovsjannikov [50] in complex form with zero surface tension and body force.

The resulting conformal ideal droplet equations form a type of water wave system with one spatial dimension, governing the time evolution of the boundary parametrization and the velocity potential at the boundary. The equations are nonlocal and nonlinear, but all nonlocality is expressed in terms of the 2π-periodic Hilbert transform H on the real line, i.e., on $\mathbb{T} = \mathbb{R}/2\pi\mathbb{Z}$.

A.1. **Ideal droplet equations.** We consider a two-dimensional drop of fluid that at time t occupies a domain Ω_t conformally equivalent to the unit disk $\mathbb{D}$ in the complex plane. We suppose the fluid is inviscid and the motion incompressible. Let $u = (u_1, u_2)$ denote the velocity field and p the pressure. We assume that the external body force $-\nabla\mathcal{V}$ is conservative, arising from a potential $\mathcal{V}$. Then inside Ω_t we have the Euler equations

$$u_t + u\cdot\nabla u + \nabla p = -\nabla\mathcal{V}, \qquad \nabla\cdot u = 0. \tag{84}$$

Assuming the flow is irrotational, the velocity must be the gradient of a potential ϕ, satisfying $u = \nabla\phi$, with ϕ harmonic in Ω_t. As is usual, because $u\cdot\nabla u = \frac{1}{2}\nabla|\nabla\phi|^2$, upon integration the Euler equations (84) yield the Bernoulli equation

$$\phi_t + \frac{1}{2}|\nabla\phi|^2 + p + \mathcal{V} = c(t) \tag{85}$$

in Ω_t, where $c(t)$ is a real constant in space. The value of p on the boundary $\partial\Omega_t$ is determined by the surface tension

$$p = \gamma\kappa, \tag{86}$$

where γ is the surface tension coefficient and κ is the (mean) curvature of $\partial\Omega_t$, chosen so the curvature of a circle is positive. The equations of motion are completed by specifying a kinematic equation which states that the normal velocity of the fluid domain Ω_t agrees with the normal component of fluid velocity $\nabla\phi$.

A.2. **Conformal mapping formulation.**

A.2.1. *Notations and basic notions.* We let (x, y) denote Eulerian coordinates inside the fluid drop Ω_t and write $z = x + iy$. The function $f = \phi + i\psi$ denotes the (holomorphic) complex velocity potential, so the Cauchy-Riemann equations $\phi_x = \psi_y$, $\phi_y = -\psi_x$ relate the stream function ψ to ϕ. The complex fluid velocity then satisfies

$$u = u_1 + iu_2 = \bar{f}_z. \tag{87}$$

We parametrize the fluid domain Ω_t at time t by a holomorphic bijection $\mathbf{Z}(\cdot,t)\colon \mathbb{D}\to\Omega_t$ denoted

$$z = \mathbf{Z}(w,t) = \mathbf{X}(w,t) + i\mathbf{Y}(w,t)\,, \qquad w\in\mathbb{D}\,.$$

In terms of the conformal variable w, the (holomorphic) velocity potential and (anti-holomorphic) velocity are written

$$\mathbf{F}(w,t) = \mathbf{\Phi}(w,t) + i\mathbf{\Psi}(w,t) = f\circ\mathbf{Z}\,, \qquad \mathbf{U}(w,t) = u\circ\mathbf{Z}\,.$$

Here the notation $f\circ\mathbf{Z}$ indicates $f(\mathbf{Z}(w,t),t)$, etc. In these terms, the relation (87) is expressed as

$$\bar{\mathbf{U}} = \frac{\mathbf{F}_w}{\mathbf{Z}_w}\,. \tag{88}$$

On the boundary $S^1 = \partial\mathbb{D}$ of the disk we write $w = e^{i\theta}$ with $\theta\in\mathbb{T} = \mathbb{R}/2\pi\mathbb{Z}$. The key dependent variables in the conformal formulation are the traces of $\mathbf{Z}$ and $\mathbf{F}$ on $\partial\mathbb{D}$, and we write

$$Z(\theta,t) = X(\theta,t) + iY(\theta,t) = \mathbf{Z}(e^{i\theta},t)\,, \qquad F(\theta,t) = \Phi(\theta,t) + i\Psi(\theta,t) = \mathbf{F}(e^{i\theta},t)\,. \tag{89}$$

A.2.2. *Fourier and Hilbert transforms.* We will write the Fourier expansion of a general square-integrable function $G\colon \mathbb{T} \to \mathbb{C}$ as

$$G(\theta) = \sum_{k\in\mathbb{Z}} \hat{G}_k e^{ik\theta}\,, \qquad \hat{G}_k = \frac{1}{2\pi}\int_{\mathbb{T}} G(\theta) e^{-ik\theta}\,d\theta\,.$$

Such a function has a holomorphic extension $\mathbf{G}$ inside the disk $\mathbb{D}$ if and only if all negative modes vanish, meaning $\hat{G}_k = 0$ for all $k < 0$. If we write

$$G = \hat{G}_0 + A + iB$$

where A and B are real, then this means $B = HA$ and $HB = -A$, where H is the Hilbert transform on $\mathbb{T}$, satisfying

$$HG(\theta) = \sum_{k\neq 0} (-i\,\operatorname{sgn} k)\hat{G}_k e^{ik\theta} = \text{p.v.}\int_{\mathbb{T}} G(s)\cot\left(\frac{\theta - s}{2}\right)\frac{ds}{2\pi}\,.$$

(Note however that $-H^2$ is not the identity on $\mathbb{T}$, unlike the Hilbert transform on $\mathbb{R}$.) Thus G has an extension $\mathbf{G}$ holomorphic in $\mathbb{D}$ exactly when $\hat{B}_k = (-i\,\operatorname{sgn} k)\hat{A}_k$ for all $k \neq 0$, and in this case

$$\mathbf{G}(w) = \sum_{k\geq 0} \hat{G}_k w^k \quad \text{for all } w \in \mathbb{D}, \qquad \hat{G}_k = \hat{A}_k + i\hat{B}_k = 2\hat{A}_k \quad \text{for all } k > 0. \tag{90}$$

A.2.3. *Choice of conformal map I.* Because of the well-known characterization of holomorphic automorphisms of the disk $\mathbb{D}$ as having the form

$$g(w) = e^{ia}\frac{\alpha - w}{1 - \bar{\alpha}w}, \qquad a \in \mathbb{T}, \quad \alpha \in \mathbb{D},$$

there is some freedom in the choice of the conformal map $\mathbf{Z}(\cdot, t)\colon \mathbb{D} \to \Omega_t$. By a well-known version of the Riemann mapping theorem [56, Theorem 3.3.1], $\mathbf{Z}$ will be uniquely determined once we specify the image of the origin

$$\mathbf{Z}_0(t) := \mathbf{Z}(0,t) = \hat{Z}_0(t) \tag{91}$$

(within the fluid domain), and the argument of the derivative $\mathbf{Z}_w(0,t)$, which we denote by $\theta_1(t)$. Using the Cauchy integral formula we calculate

$$\mathbf{Z}_w(0,t) = \frac{1}{2\pi i}\int_{S^1}\frac{\mathbf{Z}}{w^2}\,dw = \frac{1}{2\pi}\int_{\mathbb{T}} Z e^{-i\theta}\,d\theta = \hat{Z}_1(t)\,, \tag{92}$$

and observe that $\theta_1(t)$ evolves according to

$$\theta_1'(t) = \frac{d}{dt}\arg\hat{Z}_1(t) = \operatorname{Im}\frac{\hat{Z}_1'}{\hat{Z}_1}\,. \tag{93}$$

A.2.4. *Holomorphic kinematic equation.* The kinematic condition that the conformal image of $\mathbb{D}$ follows the fluid motion corresponds to the condition that the normal component of coordinate velocity $\mathbf{Z}_t$ matches that of the fluid velocity on $\partial\mathbb{D}$. Thus we should explain how $\mathbf{Z}_t$ is determined by a given normal velocity law up to conformal automorphisms of $\mathbb{D}$.

We define (non-normalized) tangent and outer normal vectors to the boundary of Ω_t by

$$\tau(\theta,t) = Z_\theta = \frac{\partial}{\partial\theta}\mathbf{Z}(e^{i\theta},t)\,, \qquad n(\theta,t) = -iZ_\theta\,. \tag{94}$$

These functions are traces on $\partial\mathbb{D}$ of the respective holomorphic functions

$$\boldsymbol{\tau}(w,t) = iw\mathbf{Z}_w\,, \qquad \boldsymbol{n}(w,t) = w\mathbf{Z}_w\,, \quad w \in \mathbb{D}\,. \tag{95}$$

Next we introduce normal and tangential components of Z_t (non-normalized) by writing

$$\bar{n}Z_t = v^n + iv^\tau\,, \qquad v^n = \operatorname{Re}\bar{n}Z_t\,, \quad v^\tau = \operatorname{Im}\bar{n}Z_t = \operatorname{Re}\bar{\tau}Z_t\,. \tag{96}$$

Because $\mathbf{Z}_t$ is holomorphic in $\mathbb{D}$, it is essentially determined by the normal component v^n up to automorphism, as follows. Because $\mathbf{Z}(\cdot,t)$ is presumed injective on $\mathbb{D}$, the derivative $\mathbf{Z}_w$ cannot vanish inside $\mathbb{D}$. (For an in-depth discussion of injectivity see subsection A.5 below.) Hence we can write

$$\mathbf{Z}_t = \mathbf{Z}_w\mathbf{G}\,, \tag{97}$$

where $\mathbf{G}$ is holomorphic in $\mathbb{D}$. Substituting into (96) and using (95), we infer that on $\partial\mathbb{D}$,

$$\frac{G}{w} = \frac{v^n}{J} + i\frac{v^\tau}{J}\,, \qquad J := \bar{n}n = |Z_\theta|^2\,. \tag{98}$$

This expression is holomorphic in $\mathbb{D}$ except for a pole at 0 with residue $\hat{G}_0 = \mathbf{G}(0,t)$. Then it follows (noting that the imaginary part of the constant term is not recovered by iH)

$$\frac{G-\hat{G}_0}{w} = (I+iH)\operatorname{Re}\left(\frac{G-\hat{G}_0}{w}\right) + i\operatorname{Im}\hat{G}_1\,. \tag{99}$$

Since $(I+iH)\operatorname{Re}(\hat{G}_0/w) = (I+iH)\operatorname{Re}(w\overline{\hat{G}_0}) = w\overline{\hat{G}_0}$ on $\partial\mathbb{D}$, we infer

$$G = w(I+iH)\operatorname{Re}\left(\frac{G}{w}\right) + v_0(\theta,t)\,, \tag{100}$$

where

$$v_0(\theta,t) = \hat{G}_0(t) + iw\operatorname{Im}\hat{G}_1(t) - w^2\overline{\hat{G}_0(t)}\,. \tag{101}$$

The formulas (100)–(101) express G clearly as the boundary trace of a holomorphic function. The coefficients $\hat{G}_0$, $\operatorname{Im}\hat{G}_1$ are associated with the choice of conformal map as expressed in (91) and (93), via the relations

$$\hat{G}_0 = \frac{\mathbf{Z}_t(0,t)}{\mathbf{Z}_w(0,t)} = \frac{\hat{Z}_0'}{\hat{Z}_1}\,, \tag{102}$$

$$\operatorname{Im}\hat{G}_1 = \operatorname{Im}\left(\frac{\mathbf{Z}_{wt}}{\mathbf{Z}_w} - \frac{\mathbf{Z}_{ww}\mathbf{Z}_t}{\mathbf{Z}_w^2}\right)_{w=0} = \theta_1'(t) - \operatorname{Im}\frac{2\hat{Z}_2\hat{Z}_0'}{\hat{Z}_1^2}\,. \tag{103}$$

In this way, $\mathbf{Z}_t$ is determined by the (non-normalized) normal velocity v^n and the functions θ_1' and $\hat{Z}_0' = \mathbf{Z}_0'$, which may be freely specified.

Finally, the physical kinematic relation requires that the normal component of $\mathbf{Z}_t$ matches that of the complex fluid velocity $\mathbf{U}$ from (88), which means simply that

$$v^n = \operatorname{Re}\boldsymbol{n}\bar{\mathbf{U}} = \operatorname{Re} w\mathbf{F}_w = \operatorname{Re}(-iF_\theta) = \Psi_\theta\,. \tag{104}$$

This then determines G as in (100) with

$$\operatorname{Re}\left(\frac{G}{w}\right) = \frac{\Psi_\theta}{J}. \tag{105}$$

A.2.5. *Holomorphic Bernoulli equation.* Because $\phi_t = \operatorname{Re} f_t$ and $|\nabla\phi|^2 = |f_z|^2$, the usual Bernoulli equation (85) reads

$$\operatorname{Re} f_t + \frac{1}{2}|f_z|^2 + p + \mathcal{V} = c(t)\,. \tag{106}$$

Recalling that $\mathbf{F}(w,t) = f(\mathbf{Z}(w,t),t)$, we compute $\mathbf{F}_t = f_t \circ \mathbf{Z} + (f_z \circ \mathbf{Z})\mathbf{Z}_t$, so that

$$\mathbf{R} := -f_t \circ \mathbf{Z} = -\mathbf{F}_t + \frac{\mathbf{F}_w \mathbf{Z}_t}{\mathbf{Z}_w} = -\mathbf{F}_t + \mathbf{F}_w \mathbf{G}\,,$$

$$\frac{1}{2}|f_z \circ \mathbf{Z}|^2 = \frac{1}{2}\left|\frac{\mathbf{F}_w}{\mathbf{Z}_w}\right|^2 = \frac{1}{2}\frac{|F_\theta|^2}{|Z_\theta|^2} = \frac{\Phi_\theta^2 + \Psi_\theta^2}{2J}\,.$$

Because $\mathbf{R}$ is holomorphic, we can use the last equation with (106) to express the Bernoulli equation in holomorphic form as

$$\mathbf{F}_t = \mathbf{F}_w \mathbf{G} - \mathbf{R}\,, \qquad R = (1+iH)\left(\frac{\Phi_\theta^2 + \Psi_\theta^2}{2J} + p + \mathcal{V}\right) + \tilde{c}(t)\,, \tag{107}$$

where $R(\theta,t) = \mathbf{R}(e^{i\theta},t)$. Inside the fluid, the pressure in conformal variables may be expressed using (106) in the form

$$p \circ \mathbf{Z} = \operatorname{Re}\mathbf{R} - \frac{1}{2}\left|\frac{\mathbf{F}_w}{\mathbf{Z}_w}\right|^2 - \mathcal{V} + c(t)\,. \tag{108}$$

A.2.6. *Choice of conformal map II.* Recall that we may freely specify $\theta_1'(t)$ (real) and $\mathbf{Z}_0'$ (complex), as long as $\mathbf{Z}_0(t)$ does not hit $\partial\Omega_t$. We discuss two choices of these functions that may be particularly useful. The simplest choice is certainly to choose

$$\theta_1'(t) = 0, \quad \mathbf{Z}_0'(t) = 0. \tag{109}$$

From (101) this is clearly equivalent to the condition

$$\upsilon_0(\theta,t) = 0. \tag{110}$$

This corresponds to what was done in [50], and can suffice for short times or symmetric flows. In order that the point $\mathbf{Z}(0,t)$ should remain inside the fluid domain over longer times, however, it may be convenient to choose $\mathbf{Z}_0(t)$ to move with the fluid velocity $\mathbf{U}_0(t) = \mathbf{U}(0,t)$, so that

$$\overline{\mathbf{Z}_0'(t)} = \bar{\mathbf{U}}_0(t) = \frac{\mathbf{F}_w(0,t)}{\mathbf{Z}_w(0,t)} = \frac{\hat{F}_1(t)}{\hat{Z}_1(t)}\,. \tag{111}$$

Then it seems simplest to choose $\theta_1' = 2\operatorname{Im}\mathbf{Z}_0'\hat{Z}_2\hat{Z}_1^{-2}$, which makes $\operatorname{Im}\hat{G}_1 = 0$. It follows

$$\upsilon(\theta,t) = \frac{w}{|\hat{Z}_1|^2}\left(\overline{w\hat{F}_1} - w\hat{F}_1\right) = \frac{-2iw\operatorname{Im}(w\hat{F}_1)}{|\hat{Z}_1|^2}\,. \tag{112}$$

A.2.7. *Real equations.* Computation and analysis are carried out in terms of the real parts of the traces $X = \operatorname{Re} Z$ and $\Phi = \operatorname{Re} F$ on the circle $\partial\mathbb{D}$, relying on the Hilbert transform to recover the imaginary parts as needed. Because $w\mathbf{Z}_w = -i\mathbf{Z}_\theta = -i(X_\theta + iY_\theta)$ on $\partial\mathbb{D}$, from (97) we get

$$X_t = \operatorname{Im}(X_\theta + iY_\theta)\left(\frac{\upsilon^n}{J} + i\frac{\upsilon^\tau}{J}\right) = Y_\theta\frac{\upsilon^n}{J} + X_\theta\frac{\upsilon^\tau}{J}\,. \tag{113}$$

Because $w\mathbf{F}_w = -iF_\theta = -i(\Phi_\theta + i\Psi_\theta)$ on $\partial\mathbb{D}$, the real part of (107) yields

$$\begin{aligned}\Phi_t &= \operatorname{Im}(\Phi_\theta + i\Psi_\theta)\left(\frac{\upsilon^n}{J} + i\frac{\upsilon^\tau}{J}\right) - \frac{\Phi_\theta^2 + \Psi_\theta^2}{2J} - p - \mathcal{V} - \tilde{c}_1(t) \\ &= \frac{1}{2J}(\Psi_\theta^2 - \Phi_\theta^2) + \Phi_\theta\frac{\upsilon^\tau}{J} - p - \mathcal{V} - \tilde{c}_1(t)\,,\end{aligned} \tag{114}$$

where to get the last equality we use the fact that $\upsilon^n = \Psi_\theta$ from (104). We typically choose $\tilde{c}_1 = 0$, but one could instead choose $\tilde{c}_1$ to enforce $\hat{\Phi}_0$ to be constant.

The pressure is given on the boundary as $p = \gamma\kappa$, where γ is the coefficient of surface tension and κ is the curvature of the curve $\theta \mapsto (X(\theta,t), Y(\theta,t))$. With the convention that the curvature of a circle is positive, the pressure at the boundary is

$$p = \gamma\frac{X_\theta Y_{\theta\theta} - X_{\theta\theta}Y_\theta}{(X_\theta^2 + Y_\theta^2)^{3/2}}. \tag{115}$$

We summarize the equations of motion in terms of X and Φ using the operator defined by

$$\Lambda = H\partial_\theta = \partial_\theta H\,, \tag{116}$$

so that $Y_\theta = HX_\theta = \Lambda X$ and $\Psi_\theta = H\Phi_\theta = \Lambda\Phi$, e.g. We compute that

$$\frac{\upsilon^\tau}{J} = \operatorname{Im}\frac{G}{w} = H\left(\frac{\upsilon^n}{J}\right) + \operatorname{Im}\left(\frac{\upsilon_0}{w}\right), \tag{117}$$

and note that

$$\frac{\upsilon_0}{w} = \bar{w}\hat{G}_0 - w\overline{\hat{G}_0} + i\operatorname{Im}\hat{G}_1 = i\operatorname{Im}(2\bar{w}\hat{G}_0 + \hat{G}_1) =: i\upsilon_1(\theta,t). \tag{118}$$

Taking $\tilde{c}_1 = 0$, we obtain the evolution equations governing ideal droplets finally in the form

$$X_t = (\Lambda X)\frac{\Lambda\Phi}{J} + X_\theta\left(H\left(\frac{\Lambda\Phi}{J}\right) + \upsilon_1\right), \tag{119}$$

$$\Phi_t = -p - \mathcal{V} + \frac{(\Lambda\Phi)^2 - \Phi_\theta^2}{2J} + \Phi_\theta\left(H\left(\frac{\Lambda\Phi}{J}\right) + \upsilon_1\right), \tag{120}$$

with the definitions

$$J = X_\theta^2 + (\Lambda X)^2\,, \qquad p = \gamma J^{-3/2}(X_\theta\,\Lambda X_\theta - X_{\theta\theta}\,\Lambda X)\,. \tag{121}$$

Remark A.1. We can always require $\Psi = H\Phi$ by choosing $\hat{\Psi}_0 = 0$. However, $HX = Y - \hat{Y}_0$, so one needs to know $\hat{Y}_0 = \mathbf{Y}(0,t)$ in order to completely reconstruct Y from X. In case one makes the simple choice $\upsilon_0 \equiv 0$, then because this is equivalent to (109), it follows that necessarily

$$\hat{X}_0'(t) = \hat{Y}_0'(t) = 0\,, \tag{122}$$

whence $\hat{X}_0(t)$ and $\hat{Y}_0(t)$ remain constant in time. In case one makes the choice (112), however, one should determine $\hat{Y}_0(t)$ by solving the equation

$$\hat{Y}_0'(t) = -\operatorname{Im}\frac{\hat{F}_1}{\hat{Z}_1} = -\operatorname{Im}\frac{\hat{\Phi}_1}{\hat{X}_1}\,, \tag{123}$$

which derives from (111) by applying (90) to $\mathbf{F}$ and $\mathbf{Z}$.

A.2.8. *Galilean invariance.* One can check (with a bit of difficulty) that the conformal equations of motion above are invariant under a Galilean transformation

$$\mathbf{Z} = \breve{\mathbf{Z}} + \boldsymbol{v}t\,, \quad \mathbf{F} = \breve{\mathbf{F}} + \bar{\boldsymbol{v}}\breve{\mathbf{Z}}\,, \qquad \boldsymbol{v} \in \mathbb{C}\,, \tag{124}$$

for which $\mathbf{U} = \breve{\mathbf{U}} + \boldsymbol{v}$, $\mathbf{Z}_0 = \breve{\mathbf{Z}}_0 + \boldsymbol{v}t$, $\mathbf{Z}_w = \breve{\mathbf{Z}}_w$, and

$$\mathbf{G} = \frac{\mathbf{Z}_t}{\mathbf{Z}_w} = \breve{\mathbf{G}} + \frac{\boldsymbol{v}}{\mathbf{Z}_w}\,.$$

Defining $\breve{\upsilon}^n$ and $\breve{\upsilon}^\tau$ by the analog of (96), we obtain the analog of (101) and (117) due to the fact that the holomorphic function $1/\mathbf{Z}_w$ has Taylor series that starts with the linear approximation

$$\frac{1}{\mathbf{Z}_w(0,t)} - \frac{\mathbf{Z}_{ww}(0,t)}{\mathbf{Z}_w(0,t)^2} w = \hat{Z}_1^{-1} - 2\hat{Z}_2\hat{Z}_1^{-2} w$$

which implies

$$\frac{\operatorname{Im} \boldsymbol{v}\bar{n}}{J} = H\left(\frac{\operatorname{Re} \boldsymbol{v}\bar{n}}{J}\right) + 2\operatorname{Im} \boldsymbol{v}(\hat{Z}_1 e^{-i\theta} - \hat{Z}_2\hat{Z}_1^{-2})\,.$$

From (96) and its analog we have

$$\upsilon^n = \operatorname{Re} \bar{n} Z_t = \operatorname{Re} \bar{n}(\breve{Z}_t + \boldsymbol{v}) = \breve{\upsilon}^n + \operatorname{Re} \bar{\boldsymbol{v}} n\,,$$

while

$$\Psi_\theta = \operatorname{Im} F_\theta = \operatorname{Im}(\breve{F}_\theta + \bar{\boldsymbol{v}} Z_\theta) = \breve{\Psi}_\theta + \operatorname{Re} \bar{\boldsymbol{v}} n\,.$$

Consequently $\breve{\upsilon}^n = \breve{\Psi}_\theta$ and the relation (104) transforms as desired.

It is then straightforward to check that the Bernoulli equation (107) transforms properly, by expanding $\frac{1}{2}|\breve{\mathbf{U}} + \boldsymbol{v}|^2$ and adjusting $\tilde{c}(t)$ to ensure that

$$\operatorname{Re} R = \operatorname{Re}\left(\breve{R} - \breve{\mathbf{U}}\bar{\boldsymbol{v}} - |\boldsymbol{v}|^2\right)\,.$$

A.3. **Geodesic paths in the conformal mapping formulation.** The governing evolution equations (119)–(120) can be derived from a variational principle (principle of stationary action) in a manner following the derivation in [19]. In [19], Dyachenko et al. started from Zakharov's canonical Hamiltonian system for water waves [62], wrote the action as the time integral of a Lagrangian, expressed this in terms of conformal variables, and set the first variation to zero.

The essence of this variational derivation is closely related to Arnold's geometric description of smooth incompressible Euler flow (in a fixed domain) as geodesic flow in the group of volume-preserving diffeomorphisms. Here we show how geodesic conditions yield the correct equations of motion in the present context of ideal droplet flows, governed by two-dimensional incompressible potential flow with zero surface tension and zero force potential, in the conformal mapping formulation. Our computation here corresponds to the computation of geodesic equations in [41] using Eulerian and Lagrangian variables.

Consider a path of conformal injections $\mathbf{Z}\colon \mathbb{D} \to \mathbb{C}$ that preserve the area of $\Omega_t = \mathbf{Z}(\mathbb{D}, t)$, given by

$$|\Omega_t| = \int_{\partial\Omega_t} x\,dy = \int_{\mathbb{T}} XY_\theta\,d\theta = \int_{\mathbb{T}} X\,\Lambda X\,d\theta = \frac{1}{2}\operatorname{Im}\int_{\mathbb{T}} \bar{Z} Z_\theta\,d\theta\,. \tag{125}$$

We formally define a 'Riemannian metric' by pulling back the Eulerian kinetic energy of the potential flow induced in Ω_t by the harmonic velocity potential ϕ whose pulled-back boundary values Φ are determined (up to constant) by $\mathbf{Z}$ and $\mathbf{Z}_t$ via (104), which we can write in the form

$$\upsilon^n = \operatorname{Re} \bar{n} Z_t = \operatorname{Im} Z_\theta \bar{Z}_t = \Psi_\theta = \Lambda\Phi\,. \tag{126}$$

We note that for the geodesic variational principle, this kinematic relation (126) is *imposed* in order to define a notion of path length corresponding to a suitable 'metric.' This entails the kinematic equation (119) by following the computations in subsection A.2.4 same as before.

In terms of the holomorphic velocity potential $\phi + i\psi$ on Ω_t and its pullback $\mathbf{\Phi} + i\mathbf{\Psi}$ on $\mathbb{D}$, the kinetic energy is half of the following quantity (where ν corresponds to the unit outer normal to $\partial\Omega_t$):

$$\int_{\Omega_t} |\nabla\phi|^2 = \int_{\partial\Omega_t} \phi\, \partial_\nu\phi\, ds = \int_{\partial\Omega_t} \phi\, \partial_s\psi\, ds = \int_{\mathbb{T}} \Phi\, \Psi_\theta\, d\theta. \tag{127}$$

We regard this as a quadratic form on the 'tangent space' of the 'manifold' of conformal images of $\mathbb{D}$, producing a 'Riemannian metric' at base point $\mathbf{Z}$ given by

$$g_{\mathbf{Z}}(\mathbf{Z}_t, \mathbf{Z}_t) = \int_{\mathbb{T}} \Phi\, \Lambda\Phi\, d\theta\,. \tag{128}$$

This 'metric' is naturally degenerate in $\mathbf{Z}_t$ because the conformal map $\mathbf{Z}$ has the same freedom as before: A different choice of $\mathbf{Z}_0'$ and $\theta_1'(t)$ corresponds to a path $\mathbf{Z}$ that differs only by right composition with a holomorphic automorphism of $\mathbb{D}$, and the image of $\mathbf{Z}$, the Eulerian flow, and the metric do not change.

A geodesic path with respect to this metric is one for which the action

$$\mathcal{A} = \int_0^T \int_{\mathbb{T}} \frac{1}{2}\Phi\, \Lambda\Phi\, d\theta\, dt$$

is stationary. The variation is

$$\delta\mathcal{A} = \int_0^T \int_{\mathbb{T}} \Phi\, \Lambda\delta\Phi\, d\theta\, dt.$$

Taking the variation of the kinematic equation (126), we find

$$\Lambda\delta\Phi = \mathrm{Im}(Z_\theta\, \overline{\delta Z}_t - Z_t\, \overline{\delta Z}_\theta)\,.$$

Substituting in and integrating by parts (requiring $\delta Z = 0$ at the endpoints $t = 0$ and $t = T$), we get

$$\delta\mathcal{A} = -\,\mathrm{Im} \int_0^T \int_{\mathbb{T}} \overline{\delta Z}(\Phi_t Z_\theta - \Phi_\theta Z_t)\, d\theta\, dt. \tag{129}$$

The variation δZ is an arbitrary holomorphic function subject to a constraint arising from fixing the area given by (125). From (125) we find the constraint on δZ takes the form

$$0 = \int_{\mathbb{T}} \delta X\, \Lambda X\, d\theta = \frac{1}{2}\,\mathrm{Im} \int_{\partial\mathbb{D}} \overline{\delta Z} Z_\theta\, d\theta\,. \tag{130}$$

Because the negative Fourier modes of δZ vanish, and the non-negative Fourier modes are arbitrary up to the orthogonality condition (130), we conclude that the factor $\Phi_t Z_\theta - \Phi_\theta Z_t$ in the integrand in (129) is anti-holomophic with mean zero (having only negative Fourier modes), modulo a real constant multiple of Z_θ. Thus for some real function $c(t)$,

$$\Phi_t Z_\theta - \Phi_\theta Z_t = \bar{Q} + c(t) Z_\theta \tag{131}$$

where $Q : \mathbb{T} \to \mathbb{C}$ which is the trace of some mean-zero holomorphic function in $\mathbb{D}$. (To see that $c(t)$ must be real, use (131) in (129) with $\delta Z = Z_\theta$.)

We isolate the factor Φ_t from this equation as follows. First, multiply by $\bar{Z}_\theta$, noting that $Z_\theta Q$ is the boundary trace of the holomorphic function $iw\mathbf{Z}_w\mathbf{Q}$ and this has zero average over S^1. Next we apply $1 + iH$ to both sides, which eliminates the term $\overline{Z_\theta Q}$ and yields

$$(1 + iH)(J\Phi_t) = (1 + iH)(\Phi_\theta \bar{Z}_\theta Z_t) + c(t)(1 + iH)J$$

From (96) and (117)–(118) we can write

$$\bar{Z}_\theta Z_t = \bar{Z}_\theta(-iZ_\theta)\left((1+iH)\frac{\Psi_\theta}{J}+i\upsilon_1\right) = J\left(H\frac{\Psi_\theta}{J}+\upsilon_1\right) - i\Psi_\theta\,.$$

Substituting this in above and taking the real part we find

$$J\Phi_t = J\Phi_\theta\left(H\frac{\Psi_\theta}{J}+\upsilon_1\right) + H(\Phi_\theta\Psi_\theta) + c(t)J. \tag{132}$$

Now, because $\Psi_\theta = H\Phi_\theta$, the function $\Phi_\theta + i\Psi_\theta$ is a holomorphic trace with mean zero. Hence so is the square of this function, and consequently

$$\Phi_\theta^2 - \Psi_\theta^2 = -H(2\Phi_\theta\Psi_\theta)\,.$$

Using this in (132) one obtains the Bernoulli equation (120) with zero surface tension γ and zero force potential $\mathcal{V}$.

A.3.1. *Surface tension and potential energy.* To include the effects of body force and surface tension in the action principle, we subtract the bulk potential energy and interfacial energy (the droplet perimeter times γ here), to obtain the modified action

$$\mathcal{A}_{\gamma,\mathcal{V}} = \int_0^T \left(\int_{\mathbb{T}}\left(\frac{1}{2}\Phi\,\Lambda\Phi - \gamma|Z_\theta|\right)d\theta - \int_{\Omega_t}\mathcal{V}(z)\,dx\,dy\right)dt\,, \quad \Omega_t = \mathbf{Z}(\mathbb{D},t)\,. \tag{133}$$

To determine the variation of bulk potential energy we proceed as follows. Because a virtual displacement δZ corresponds to virtual normal velocity

$$\tilde{v}_\nu := \operatorname{Re}\overline{\delta Z}\left(\frac{-iZ_\theta}{|Z_\theta|}\right) = \operatorname{Im}\overline{\delta Z}\frac{Z_\theta}{|Z_\theta|},$$

using the Reynolds transport theorem we compute

$$\delta\int_{\Omega_t}\mathcal{V}(z)\,dx\,dy = \int_{\partial\Omega_t}\mathcal{V}(z)\tilde{v}_\nu\,ds = \operatorname{Im}\int_{\mathbb{T}}\overline{\delta Z}\,\mathcal{V}(Z)Z_\theta\,d\theta.$$

The variation of droplet perimeter is given by

$$\delta\int_{\partial\Omega_t}1\,ds = \delta\int_{\mathbb{T}}|Z_\theta|\,d\theta = \operatorname{Re}\int_{\mathbb{T}}\overline{\delta Z}_\theta\frac{Z_\theta}{|Z_\theta|}\,d\theta = -\operatorname{Im} i\int_{\mathbb{T}}\overline{\delta Z}\left(\frac{Z_\theta}{|Z_\theta|}\right)_\theta d\theta.$$

Because $Z_\theta/|Z_\theta|$ is a unit tangent vector to $\partial\Omega_t$ and $ds = |Z_\theta|\,d\theta$, we have $i(Z_\theta/|Z_\theta|)_\theta = -\kappa Z_\theta$ where κ is the curvature of $\partial\Omega_t$.

By consequence, we find

$$\delta\mathcal{A}_{\gamma,\mathcal{V}} = -\operatorname{Im}\int_0^T\int_{\mathbb{T}}\overline{\delta Z}(\Phi_t Z_\theta - \Phi_\theta Z_t + (\gamma\kappa+\mathcal{V}(Z))Z_\theta)\,d\theta\,dt, \tag{134}$$

Arguing as before, if this vanishes for all holomorphic δZ constrained by (130), then we obtain (131) with the term $(\gamma\kappa+\mathcal{V})Z_\theta$ added on the left-hand side:

$$\Phi_t Z_\theta - \Phi_\theta Z_t + (\gamma\kappa+\mathcal{V})Z_\theta = \bar{Q} + c(t)Z_\theta\,. \tag{135}$$

We then get (132) with the added term $(\gamma\kappa+\mathcal{V})J$, and (120) follows as desired.

Remark A.2. The fact that the potential energy terms in (133) appear with a negative sign is natural due to the origin of this action from Lagrangian mechanics.

A.4. **Formal conservation laws for area and energy.** The equations of motion imply conservation of the area $|\Omega_t|$, because from (125) and (126) it follows

$$\frac{d}{dt}|\Omega_t| = \frac{1}{2}\int_{\mathbb{T}} \Psi_\theta \, d\theta = 0. \tag{136}$$

The variational calculations in the previous subsection also make it convenient to establish conservation of the total (kinetic plus potential) energy given by

$$\mathcal{E} = \int_{\mathbb{T}} \left(\frac{1}{2}\Phi\,\Lambda\Phi + \gamma|Z_\theta| \right) d\theta + \int_{\Omega_t} \mathcal{V}(z)\, dx\, dy\,. \tag{137}$$

For, taking $\delta Z = Z_t$ in the potential energy computations we find

$$\partial_t \left(\int_{\mathbb{T}} \gamma|Z_\theta|\, d\theta + \int_{\Omega_t} \mathcal{V}(z)\, dx\, dy \right) = \operatorname{Im} \int_{\mathbb{T}} \bar{Z}_t Z_\theta (\gamma\kappa + \mathcal{V})\, d\theta \tag{138}$$

while, due to (126),

$$\partial_t \int_{\mathbb{T}} \frac{1}{2}\Phi\,\Lambda\Phi\, d\theta = \operatorname{Im} \int_{\mathbb{T}} \Phi_t Z_\theta \bar{Z}_t\, d\theta\,. \tag{139}$$

Adding these equations and using (135) we get

$$\frac{d\mathcal{E}}{dt} = \operatorname{Im} \int_{\mathbb{T}} (\Phi_\theta Z_t + \bar{Q} + c(t) Z_\theta) \bar{Z}_t \, d\theta = 0\,,$$

because the first term is real, the second term is anti-holomorphic with mean zero, and in the third term $c(t)$ is real and $\operatorname{Im} Z_\theta \bar{Z}_t = \Psi_\theta$, which integrates to zero.

A.5. **Criteria for continuation of conformal injectivity.** We have derived the evolution equations in (119)–(120) under the assumption that $\mathbf{Z}(\cdot, t)$ remains a conformal injection on the interval of time being considered. One would then like to have a criterion which guarantees that having a regular solution of the evolution equations on this interval of time ensures that the maps $\mathbf{Z}(\cdot, t)$ constructed by holomorphic extension from $\partial\mathbb{D}$ in fact remain conformal injections in $\mathbb{D}$.

Of course we should assume that $\mathbf{Z}$ is a conformal injection at the initial time $t = 0$. Suppose $Z = X + iY$ is C^1 on $\mathbb{T} \times [0, T]$ with $HX = Y - \hat{Y}_0$, and let $\mathbf{Z}$ be the holomorphic extension of Z into $\mathbb{D}$. If one assumes $J = |Z_\theta| > 0$ on $\mathbb{T} \times [0, T]$, say, then it follows from the maximum modulus principle and a continuation argument that $1/\mathbf{Z}_w$ remains holomorphic and bounded on $\mathbb{D} \times [0, T]$. Then $\boldsymbol{Z}_w$ will not vanish in $\mathbb{D}$, which is necessary for the map $w \mapsto \mathbf{Z}(w, t)$ to be a conformal injection.

This local condition is in principle not sufficient to ensure the global injectivity of $\mathbf{Z}$ on $\mathbb{D}$. Non-injectivity of $\mathbf{Z}(\cdot, t)$ may develop due to collision of points on the boundary, as in a so-called 'splash singularity' (see [9]). We can state a precise sufficient criterion for the continuation of injectivity as follows, making use of known results in complex function theory.

Theorem A.3 (Persistence of injectivity)**.** *Let* $\mathbf{Z}\colon \bar{\mathbb{D}} \times [0, T] \to \mathbb{C}$*, with* $\mathbf{Z}(\cdot, t)$ *holomorphic in* $\mathbb{D}$ *for each* t*, and assume* $\mathbf{Z}$ *and* $\mathbf{Z}_w$ *are continuous on* $\bar{\mathbb{D}} \times [0, T]$*. Further, assume that* $\mathbf{Z}(\cdot, 0)$ *is injective on* $\partial\mathbb{D}$*. Define*

$$T_* = \sup\{T_1 : \mathbf{Z}(\cdot, t) \text{ is injective on } \bar{\mathbb{D}} \text{ for all } t \in [0, T_1]\}.$$

Then if $T_* < T$*, the curve* $\mathbf{Z}(\partial\mathbb{D}, T_*)$ *fails to be a Jordan curve of class* $C^{1,\alpha}$ *for every* $\alpha \in (0, 1]$*.*

The point of this result is that persistence of injectivity in $\mathbb{D}$ is ensured by good behavior of the boundary trace Z. This is rather subtle since injectivity does not in principle require nonvanishing of $\boldsymbol{Z}_w$ on the boundary.

Proof. 1. Due to the classical Darboux-Picard theorem [6, Thm. 9.16, p. 310], the injectivity of $\mathbf{Z}(\cdot,t)$ on $\partial\mathbb{D}$ implies the injectivity of $\mathbf{Z}(\cdot,t)$ on $\bar{\mathbb{D}}$, for any $t \in [0,T]$. By consequence $T_* \geq 0$. Suppose that $T_* < T$. If $\mathbf{Z}(\cdot,T_*)$ is not injective on $\partial\mathbb{D}$ then it is not a Jordan curve and we are done, so assume it is injective. Then as above $\mathbf{Z}(\cdot,T_*)$ is a conformal injection on $\bar{\mathbb{D}}$.

2. Now suppose for the sake of contradiction that $\mathbf{Z}(\partial\mathbb{D},T_*)$ is a Jordan curve of class $C^{1,\alpha}$ for some $\alpha \in (0,1)$. Then, as remarked by Pascu & Pascu [52, Remark 2.2], results in the book of Pommerenke [54, p. 24 and pp. 48-49] imply that the derivative $\mathbf{Z}_w(\cdot,T_*)$ is nonvanishing on $\bar{\mathbb{D}}$. By consequence, the quantity defined by

$$K = \inf_{\substack{w_1,w_2\in\bar{\mathbb{D}}\\ w_1\neq w_2}} \left| \frac{\mathbf{Z}(w_1,T_*)-\mathbf{Z}(w_2,T_*)}{w_1-w_2} \right|, \tag{140}$$

is strictly positive, satisfying $K > 0$.

3. Now, for any function $\mathbf{Y}$ holomorphic on $\mathbb{D}$ and continuous on $\bar{\mathbb{D}}$ that satisfies

$$\hat{K} = \sup_{w\in\mathbb{D}} |\mathbf{Y}_w(w) - \mathbf{Z}_w(w,T_*)| < K\,,$$

necessarily $\mathbf{Y}$ is injective on $\bar{\mathbb{D}}$. For if $\mathbf{Y}(w_0) = \mathbf{Y}(w_1)$ for some $w_0 \neq w_1$ in $\bar{\mathbb{D}}$, then with $w_t = (1-t)w_0 + tw_1$ we have

$$|\mathbf{Z}(w_1,T_*) - \mathbf{Z}(w_0,T_*)| \leq \int_0^1 |\mathbf{Z}_w(w_t,T_*) - \mathbf{Y}_w(w_t)|\,dt\,|w_1-w_0| \leq \hat{K}|w_1-w_0|$$

and this leads to a contradiction with the definition of K. (A more subtle related argument is made in the proof of Theorem 2.4 of [52].)

4. Our assumptions ensure that we may take $\mathbf{Y} = \mathbf{Z}(\cdot,t)$ whenever $t - T_* > 0$ is sufficiently small. This contradicts the definition of T_* and concludes the proof. □

To relate this criterion back to the solution (X,Φ) of (119)–(120), we note the following corollary which is implied by the fact that the Hilbert transform is bounded on spaces $C^\alpha(\mathbb{T})$ of Hölder continuous functions, and if the map $\theta \mapsto Z(\theta,t)$ is $C^{1,\alpha}$ *with nonvanishing derivative* then the curve $Z(\mathbb{T},t)$ is $C^{1,\alpha}$.

Corollary A.4. *Suppose $X \in C([0,T],C^{1,\alpha}(\mathbb{T}))$ for some $\alpha \in (0,1)$ and $\mathbf{Z}$ is the holomorphic extension of $Z = X+iHX$ into $\mathbb{D}$. Then $\mathbf{Z} \in C([0,T],C^{1,\alpha}(\bar{\mathbb{D}}))$. Assume moreover that $Z(\cdot,0)$ is injective on $\mathbb{T}$ and define T_* as in the previous Theorem. Then if $T_* < T$, either $Z(\cdot,T_*)$ is not injective on $\mathbb{T}$, or $|Z_\theta(\theta_*,T_*)| = 0$ for some $\theta_* \in \mathbb{T}$.*

Remark A.5. We note that in recent work of Kinsey and Wu [34] and Wu [61], certain types of free-surface corners present in the initial data have been shown to persist for short time in solutions of water wave equations. The results above would say nothing about conformal parametriztions of such solutions, since the interface would fail to be $C^{1,\alpha}$ at all times.

References

[1] V. Arnold, *Sur la géométrie différentielle des groupes de Lie de dimension infinie et ses applications à l'hydrodynamique des fluides parfaits*, Ann. Inst. Fourier (Grenoble), 16 (1966), pp. 319–361.

[2] J. Beale, T. Hou, and J. Lowengrub, *Growth rates for the linearized motion of fluid interfaces away from equilibrium*, Commun. Pur. Appl. Math., 46 (1993), pp. 1269–1301.

[3] A. V. Borisov, A. A. Kilin, and I. S. Mamaev, *The Hamiltonian dynamics of self-gravitating liquid and gas ellipsoids*, Regul. Chaotic Dyn., 14 (2009), pp. 179–217.

[4] H. Bredmose, A. Hunt-Raby, R. Jayaratne, and G. N. Bullock, *The ideal flip-through impact: experimental and numerical investigation*, J. Engrg. Math., 67 (2010), pp. 115–136.

[5] Y. Brenier, *Minimal geodesics on groups of volume-preserving maps and generalized solutions of the Euler equations*, Comm. Pure Appl. Math., 52 (1999), pp. 411–452.
[6] R. B. Burckel, *An introduction to classical complex analysis. Vol. 1*, vol. 82 of Pure and Applied Mathematics, Academic Press, Inc. [Harcourt Brace Jovanovich, Publishers], New York-London, 1979.
[7] A. Castro, D. Córdoba, C. Fefferman, F. Gancedo, and J. Gómez-Serrano, *Finite time singularities for the free boundary incompressible Euler equations*, Ann. of Math. (2), 178 (2013), pp. 1061–1134.
[8] A. Castro, D. Córdoba, C. L. Fefferman, F. Gancedo, and J. Gómez-Serrano, *Splash singularity for water waves*, Proc. Natl. Acad. Sci. USA, 109 (2012), pp. 733–738.
[9] ———, *Splash singularity for water waves*, Proc. Natl. Acad. Sci. USA, 109 (2012), pp. 733–738.
[10] D. Chalikov and D. Sheinin, *Numerical modeling of surface waves based on principal equations of potential wave dynamics*. Technical Note NOAA/NCEP/OMB, 1996, 54 pp.
[11] S. Chandrasekhar, *Ellipsoidal figures of equilibrium*, (1969).
[12] W. Choi and R. Camassa, *Exact evolution equations for surface waves*, J. Engr. Mech., 125 (1999), pp. 756–760. 12th ASCE Engr. Mech. Conf., La Jolla, CA, MAY 17-20, 1998.
[13] M. Cooker and D. Peregrine, *Computations of violent motion due to waves breaking against a wall*, in Proc. 22nd Intl. Conf. on Coastal Engineering, ASCE, 1990, pp. 164–176.
[14] ———, *Violent motion as near breaking waves meet a vertical wall*, in Breaking waves, Springer, 1992, pp. 291–297. IUTAM Symposium Sydney/Australia 1991.
[15] D. Coutand and S. Shkoller, *Well-posedness of the free-surface incompressible Euler equations with or without surface tension*, J. Amer. Math. Soc., 20 (2007), pp. 829–930.
[16] ———, *A simple proof of well-posedness for the free-surface incompressible Euler equations*, Discrete Contin. Dyn. Syst. Ser. S, 3 (2010), pp. 429–449.
[17] R. Dautray and J.-L. Lions, *Mathematical analysis and numerical methods for science and technology. Vol. 3*, Springer-Verlag, Berlin, 1990. Spectral theory and applications, With the collaboration of Michel Artola and Michel Cessenat, Translated from the French by John C. Amson.
[18] P. G. L. Dirichlet, *Untersuchungen über ein Problem der Hydrodynamik*, vol. 8, Dieterichschen Buchhandlung, 1860.
[19] A. Dyachenko, E. Kuznetsov, M. Spector, and V. Zakharov, *Analytical description of the free surface dynamics of an ideal fluid (canonical formalism and conformal mapping)*, Phys. Lett. A, 221 (1996), pp. 73–79.
[20] A. I. Dyachenko, *On the dynamics of an ideal fluid with a free surface*, Doklady Mathematics, 63 (2001), pp. 115–117.
[21] A. I. Dyachenko, V. E. Zakharov, and E. A. Kuznetsov, *Nonlinear dynamics of the free surface of an ideal fluid*, Plasma Phys. Rep., 22 (1996), pp. 829–840.
[22] S. Dyachenko and A. C. Newell, *Whitecapping*, Stud. Appl. Math., 137 (2016), pp. 199–213.
[23] S. A. Dyachenko, *On the dynamics of a free surface of an ideal fluid in a bounded domain in the presence of surface tension*, J. Fluid Mech., 860 (2019), pp. 408–418.
[24] S. A. Dyachenko, P. M. Lushnikov, and A. O. Korotkevich, *Branch cuts of Stokes wave on deep water. Part I: Numerical solution and Padé approximation*, Stud. Appl. Math., 137 (2016), pp. 419–472.
[25] R. Fitzpatrick, *Theoretical Fluid Mechanics*, 2053-2563, IOP Publishing, 2017.
[26] J. E. Hogrefe, N. L. Peffley, C. L. Goodridge, W. T. Shi, H. G. E. Hentschel, and D. P. Lathrop, *Power-law singularities in gravity-capillary waves*, Phys. D, 123 (1998), pp. 183–205. Nonlinear waves and solitons in physical systems (Los Alamos, NM, 1997).
[27] T. Y. Hou and R. Li, *Computing nearly singular solutions using pseudo-spectral methods*, J. Comput. Phys., 226 (2007), pp. 379–397.
[28] J. K. Hunter, M. Ifrim, and D. Tataru, *Two dimensional water waves in holomorphic coordinates*, Comm. Math. Phys., 346 (2016), pp. 483–552.
[29] M. I., *Elliptic functions for matlab and octave*. `https://github.com/moiseevigor/elliptic`, 2008.
[30] F. John, *Two-dimensional potential flows with a free boundary*, Comm. Pure Appl. Math., 6 (1953), pp. 497–503.
[31] T. Kano and T. Nishida, *Sur les ondes de surface de l'eau avec une justification mathématique des équations des ondes en eau peu profonde*, J. Math. Kyoto Univ., 19 (1979), pp. 335–370.
[32] E. A. Karabut and E. N. Zhuravleva, *Unsteady flows with a zero acceleration on the free boundary*, J. Fluid Mech., 754 (2014), pp. 308–331.
[33] ———, *Reproduction of solutions in the plane problem on motion of a free-boundary fluid*, Doklady Physics, 61 (2016), pp. 347–350.

[34] R. H. Kinsey and S. Wu, *A priori estimates for two-dimensional water waves with angled crests*, Camb. J. Math., 6 (2018), pp. 93–181.
[35] H. Lamb, *Hydrodynamics*, Cambridge Mathematical Library, Cambridge University Press, Cambridge, sixth ed., 1993. With a foreword by R. A. Caflisch [Russel E. Caflisch].
[36] O. M. Lavrenteva, *Motion of a liquid ellipsoid*, Dokl. Akad. Nauk SSSR, 253 (1980), pp. 828–831.
[37] D. Lewis, *Relative critical points*, SIGMA Symmetry Integrability Geom. Methods Appl., 9 (2013), Paper 038, 28 pp.
[38] H. Lindblad, *Well-posedness for the motion of an incompressible liquid with free surface boundary*, Ann. of Math. (2), 162 (2005), pp. 109–194.
[39] R. Lipschitz, *Reduction der Bewegung eines flüssigen homogenen Ellipsoids auf das Variationsproblem eines einfachen Integrals, und Bestimmung der Bewegung für den Grenzfall eines unendlichen elliptischen Cylinders*, J. Reine Angew. Math., 78 (1874), pp. 245–272.
[40] J.-G. Liu and R. L. Pego, *On local singularities in ideal potential flows with free surface*, Chin. Ann. Math. Ser. B, 40 (2019), pp. 925–948.
[41] J.-G. Liu, R. L. Pego, and D. Slepčev, *Least action principles for incompressible flows and geodesics between shapes*, Calc. Var. Partial Differential Equations, 58 (2019), Paper No. 179, 43 pp.
[42] M. S. Longuet-Higgins, *A class of exact, time-dependent, free-surface flows*, J. Fluid Mech., 55 (1972), pp. 529–543.
[43] ———, *Self-similar, time-dependent flows with a free surface*, J. Fluid Mech., 73 (1976), pp. 603–620.
[44] M. S. Longuet-Higgins, *On the forming of sharp corners at a free surface*, Proc. Roy. Soc. London Ser. A, 371 (1980), pp. 453–478.
[45] ———, *Bubbles, breaking waves and hyperbolic jets at a free surface*, J. Fluid Mech., 127 (1983), pp. 103–121.
[46] P. M. Lushnikov, S. A. Dyachenko, and D. A. Silantyev, *New conformal mapping for adaptive resolving of the complex singularities of Stokes wave*, Proc. A., 473 (2017), pp. 20170198, 19.
[47] P. J. Morrison, N. R. Lebovitz, and J. A. Biello, *The Hamiltonian description of incompressible fluid ellipsoids*, Ann. Physics, 324 (2009), pp. 1747–1762.
[48] Z. Nehari, *Conformal mapping*, Dover Publications, Inc., New York, 1975. Reprinting of the 1952 edition.
[49] L. V. Ovsjannikov, *A plane problem on the unsteady motion of an incompressible fluid with a free boundary*, Dinamika Splošn. Sredy, (1971), pp. 22–26 (1972).
[50] ———, *A plane problem on the unsteady motion of an incompressible fluid with a free boundary*, Dinamika Splošn. Sredy, (1971), pp. 22–26 (1972).
[51] E. Padova, *Sul moto di un ellissoide fluido ed omogeneo*, Ann. Scuola Norm. Sup. Pisa Cl. Sci., 1 (1871), pp. 1–87.
[52] M. N. Pascu and N. R. Pascu, *Neighbourhoods of univalent functions*, Bull. Aust. Math. Soc., 83 (2011), pp. 210–219.
[53] D. H. Peregrine, *Water-wave impact on walls*, in Annual review of fluid mechanics, Vol. 35, vol. 35 of Annu. Rev. Fluid Mech., Annual Reviews, Palo Alto, CA, 2003, pp. 23–43.
[54] C. Pommerenke, *Boundary behaviour of conformal maps*, vol. 299 of Grundlehren der Mathematischen Wissenschaften [Fundamental Principles of Mathematical Sciences], Springer-Verlag, Berlin, 1992.
[55] B. Riemann, *Ein Beitrag zu den Untersuchungen über die Bewegung eines flüssigen gleichartigen Ellipsoides*, vol. 1, Verlag der Dieterichschen Buchhandlung, 1861.
[56] E. M. Stein and R. Shakarchi, *Complex analysis*, vol. 2, Princeton University Press, 2010.
[57] G. Taylor, *The instability of liquid surfaces when accelerated in a direction perpendicular to their planes. I*, Proc. Roy. Soc. London. Ser. A., 201 (1950), pp. 192–196.
[58] A. Wang, C. M. Ikeda-Gilbert, J. H. Duncan, D. P. Lathrop, M. J. Cooker, and A. M. Fullerton, *The impact of a deep-water plunging breaker on a wall with its bottom edge close to the mean water surface*, J. Fluid Mech., 843 (2018), pp. 680–721.
[59] S. Wu, *Well-posedness in Sobolev spaces of the full water wave problem in 2-D*, Invent. Math., 130 (1997), pp. 39–72.
[60] ———, *Well-posedness in Sobolev spaces of the full water wave problem in 3-D*, J. Amer. Math. Soc., 12 (1999), pp. 445–495.
[61] ———, *A blow-up criteria and the existence of 2d gravity water waves with angled crests*. 2015.
[62] V. Zakharov, *Stability of periodic waves of finite amplitude on the surface of a deep fluid*, J. Appl. Mech. Tech. Phy., 9 (1968), pp. 190–194.

[63] V. E. Zakharov, *Integration of a deep fluid equation with a free surface.*, Theoretical & Mathematical Physics, 202 (2020).
[64] B. W. Zeff, B. Kleber, J. Fineberg, and D. P. Lathrop, *Singularity dynamics in curvature collapse and jet eruption on a fluid surface*, Nature, 403 (2000), p. 401.
[65] E. N. Zhuravleva, N. M. Zubarev, O. V. Zubareva, and E. Karabut, *A new class of exact solutions in the planar nonstationary problem of motion of a fluid with a free boundary.*, Theoretical & Mathematical Physics, 202 (2020).
[66] N. M. Zubarev and E. A. Karabut, *Exact Local Solutions for the Formation of Singularities on the Free Surface of an Ideal Fluid*, JETP Lett., 107 (2018), pp. 412–417.